EXPERIMENTAL STUDIES OF CONVERSION COEFFICIENTS IN SOME DEFORMED NUCLEI

Thesis by

William Farrell Edwards

In Partial Fulfillment of the Requirements

For the Degree of

Doctor of Philosophy

California Institute of Technology

Pasadena, California

1960

ACKNOWLEDGMENTS

I gratefully acknowledge the financial aid given by the Atomic Energy Commission, the Schlumberger Foundation, and the National Science Foundation.

I am deeply indebted to Professor Jesse W. M. DuMond, who has given constant encouragement and aid.

Professor Felix Boehm has given excellent supervision and advice for which I am grateful.

I wish to thank Dr. Charles J. Gallagher and Dr. Geoffery Manning, with whom I was privileged to have a close scientific association.

I also acknowledge the assistance of Mssrs. Edward Seppi, Andrew L. Lebor, and Richard Cohen in some of the phases of this study.

Dr. E. Richard Cohen was very kind in providing information regarding the least-squares method.

I sincerely appreciate the efforts of Dr. Gerard Nijgh who read the manuscript and offered many helpful suggestions.

And finally, to my wife, Ann, who not only gave encouragement and forebearance, but also was of invaluable assistance in the preparation of this thesis.

ABSTRACT

The Mark I curved-crystal spectrometer at the California Institute of Technology was calibrated for intensity measurements. The predominant correction to the relative intensities is due to the energy dependent reflectivity of the curved quartz crystal which was found to vary as $E^{-1.987 \pm 0.022}$ over the energy range 60 kev $\leq E \leq$ 400 kev.

Conversion coefficients and energies of transitions in the following deformed nuclei were measured: Hf^{180}, W^{182}, W^{183}, and Re^{187}. Three E1 transitions with anomalous conversion coefficients were studied. The $(L_I + L_{II})$, L_{III}, and M coefficients of the K-forbidden 57.54-kev transition in Hf^{180} were found to be 0.458 $\pm$ 0.036, 0.084 $\pm$ 0.012, and 0.134 $\pm$ 0.015 respectively as compared with the theoretical E1 values of Rose (6) of 0.163, 0.062, and 0.086. The anomalous nature of the 152.41-kev transition in W^{182} is confirmed with the present value of the K-conversion coefficient of 0.05. The theoretical E1 value is 0.11. The K-conversion coefficient of the 72.00-kev transition in Re^{187} is $1.01\ ^{+0.14}_{-0.20}$ whereas the theoretical E1 value is 0.52. This anomaly might be explained by the fact that the transition energy differs from the K binding energy by only 0.34 kev.

The four E2 transitions in Hf^{180} show slight deviations from the theory. With the exception of the 93.33-kev transition the K-conversion coefficients are all about 10% low. Furthermore, with respect to the theoretical values, the L coefficients seem to follow a fairly smooth curve, decreasing as a function of energy and having a maximum deviation from the theoretical values of 12%.

EXPERIMENTAL STUDIES OF CONVERSION COEFFICIENTS IN SOME DEFORMED NUCLEI

Table of Contents

EXPERIMENTAL STUDIES OF CONVERSION COEFFICIENTS OF SOME DEFORMED NUCLEI

I. INTRODUCTION

The technique of using measurements of internal conversion coefficients of nuclear transitions to determine the multipolarity of each transition has been in use for over a decade. The internal conversion process, whereby an orbital electron receives the de-excitation energy in a nuclear transition, with the ejection of the electron from the atom, generally occurs in competition with gamma-ray emission. Electrons from any shell in the atom may by ejected if the transition energy is greater than their binding energy. Thus the K-conversion coefficient, α_K, is defined as the number of K electron ejections per gamma-ray emission. The conversion process is primarily dependent upon the electron wave function with contributions from the nuclear wave function generally being small. Thus, from simple "static" models of the nucleus and a knowledge of the electron wave functions, theoretical predictions of conversion coefficients as a function of transition energy, multipolarity, and atomic number may be made. When compared with experiment, these theoretical coefficients become a useful tool in the determination of transition multipolarities which in turn give information concerning the spin and parity differences in nuclear level schemes.

As techniques, both theoretical and experimental, have been refined, it has become clear that nuclear structural contributions to the conversion process are not negligible. The conversion coefficients calculated by Rose et al. (1) assuming a point nucleus were shown to be in error, in some cases by amounts that could be as large as 30% or more. Wapstra and Nijgh (2) investigated a number of M1 conversion coefficients that seemed to be discrepant and concluded that the errors were in the

theoretical values. They suggested that a correction for the influence of the finite nuclear size of the magnitude as arrived at by Sliv and Listengarten (3) (4) would account for the discrepancy. The conversion coefficient tables of Sliv and Band (5), and later the revised tables of Rose (6) that were computed with models of a nucleus of finite spacial extension show a marked deviation from the earlier point-nucleus values, especially for magnetic dipole transitions.

Church and Weneser (7) have pointed out that deviations of the nuclear structure from assumed models might cause further variations. Recently Green and Rose (8) gave a method for calculating nuclear structure effects. They separated the effects into a "static" effect and a "dynamic" effect. The static effect assumes the nucleus to be a sphere of constant charge density with contributions to the conversion process being expressed in terms of the electron wave function. The "dynamic" effect includes the nuclear wave function contribution and is therefore dependent upon the specific nuclear model used in the calculations. The coefficients by Sliv and Band (5) were calculated assuming nuclear currents confined to the surface. Shell model wave functions were used by Kisslinger (9) to calculate the dynamic effects upon conversion coefficients. Thus it is seen that precision conversion coefficient data have begun to provide information pertaining not only to transition multipolarities but also to the structure of the nucleus.

Conversion coefficients which are of particular interest for showing nuclear structure effects are those measured in isotopes in the highly deformed regions where the nucleus assumes a spheroidal shape. These regions are $A = 25$, $150 \leq A \leq 190$, and $A \geq 230$. In these regions the transitions may be highly retarded over single-particle estimates, and conversion coefficients for these hindered transitions may deviate

considerably from those predicted by theories which do not take into consideration the detailed nuclear structure.

In Hf^{180m}, for example, where the retardation factor for the forbidden 57-kev E1 transition is 10^{15}, the L-subshell pattern has been reported as anomalous with L_I too high (10) (11). In the heavy element region the 267-kev E1 transition in Np^{237}, which has a retardation over single-particle estimates of 5.5×10^8, has a K-conversion coefficient that is probably high by a factor of 10. Ta^{181} has a 482-kev M1 transition retarded by a factor of 2.6×10^6 and α_K is high by a factor greater than 2. The anomalous conversion coefficients in these deformed nuclei deviate very markedly from the estimates according to Sliv's and Rose's models. Anomalies which are not as great would also be interesting, but the precision necessary to detect them is of course greater.

It thus becomes desirable, both for transition multipolarity assignments and nuclear structure data, to couple high resolution spectroscopy with precise beta- and gamma-ray intensity measurements.

Conversion electron intensities are measured in beta spectrometers of various types (12). Most of these instruments have sufficient resolution; reliable intensity measurements can usually be made without having to apply numerous corrections. Generally, the only correction that need be made is for the transmission of the window of the Geiger counter detector. Relative electron intensities can be measured with an uncertainty that is often of the order of a few percent and seldom worse than ten or fifteen percent.

On the other hand, the determination of relative gamma-ray intensities usually involves numerous corrections arising from absorption phenomena, efficiency of the NaI (Tl) crystal detector, and other causes. Most of these corrections can easily be made and result in good measure-

ments in decay schemes with relatively few gamma rays when using conventional sodium iodide spectroscopy. However, where sources emit gamma rays whose energy difference is smaller than, or of the order of, the resolution of the spectrometer, conventional scintillation spectroscopy becomes difficult and line decomposition uncertainties enter. In many cases higher resolution is called for.

Improved resolution is presently provided by one of two methods: (1) external conversion of the gamma rays with subsequent detection by beta spectrometers and (2) crystal diffraction. The method used in this investigation was crystal diffraction.

A serious difficulty with the curved-crystal diffraction method has been due to the very strong energy dependence of the reflectivity of the crystal and has, in the past, necessitated a very large uncertainty assignment in the relative intensities of gamma-rays differing to any great extent in energy. Uncertainties from this source were often as high as 30% and sometimes as great as a factor of two. It was therefore first necessary to determine this dependence more precisely in order to capitalize on the high resolution of the bent crystal spectrometer. This has been done with the result that for the (310) planes in a quartz slab 2mm thick, and bent to a 2 meter radius of curvature, the reflectivity of the crystal was found to vary as $E^{-1.987 \pm 0.022}$. The uncertainty in the exponent reflects a relative intensity uncertainty of only 3% with gamma rays differing by a factor of 4 in energy.

With the reflection coefficient variation determined and an overall intensity calibration of the gamma-ray spectrometer completed, studies were made of conversion coefficients in the rare-earth region. The deformed nuclei chosen were Hf^{180}, Re^{187}, W^{182}, and W^{183}. The first named was interesting because of the highly retarded E1 transition from

the isomeric state in Hf^{180m}. In addition, the energy levels of this nucleus were studied and the application of the two parameter rotational formula to these levels shows a discrepancy from the theoretically predicted values.

In addition to conversion coefficients in the deformed Re^{187} nucleus, the study of the decay of W^{187} gave new information pertaining to the decay scheme and transition multipolarities.

Gamma-ray intensities of transitions in W^{182} and W^{183} were remeasured because of the large uncertainties in these quantities which had previously been measured in this laboratory (13).

Important information which has been gathered as a result of this study but which does not directly pertain to the principal topic of this thesis is found in the appendices.

Part II

INSTRUMENTS, TECHNIQUES, AND SOURCE PREPARATION

The primary instruments used in this study were the Mark I curved-crystal gamma-ray spectrometer, the ring-focusing magnetic beta-ray spectrometer, and the semi-circular beta-ray spectrometer, all of which are designs especially developed at the California Institute of Technology. A very brief description of the instruments will follow.

A. Curved-crystal Spectrometer

The operation of the curved-crystal gamma-ray spectrometer is well described in the literature (14) (15); therefore, it will be but briefly reviewed here. Referring to Fig. 1, the important parts of the spectrometer which will be mentioned in this paper are as follows: R is the position of the gamma-ray source which is situated on the focal circle F. The path of the gamma rays is from the source, R, to the curved crystal, C, through the collimator, D, and finally to the detector, A. As the rays are incident on the planes of the transmission type crystal at angle, θ, they are diffracted at that same angle provided they have the wavelength appropriate to that angle in accord with the Bragg relation

$$n \lambda = 2 d \sin \theta \quad . \qquad (1)$$

The geometry is designed so that the heavy collimator and the detector are fixed while the crystal moves with angular speed, ω, and the source with angular speed, 2ω, about the crystal pivot. The quartz crystal used was a slab 2 mm thick cut so that the (310) planes were used to diffract the radiation.

The wavelength of a spectral line is found by measuring the intensity of the line as a function of θ and applying Bragg's law (Eq. 1) to the angle representing the peak of the diffracted line. Actually, the instrument is designed to measure $\sin\theta$ rather than θ . This is a great simplification for the operator; since the position scale corresponds

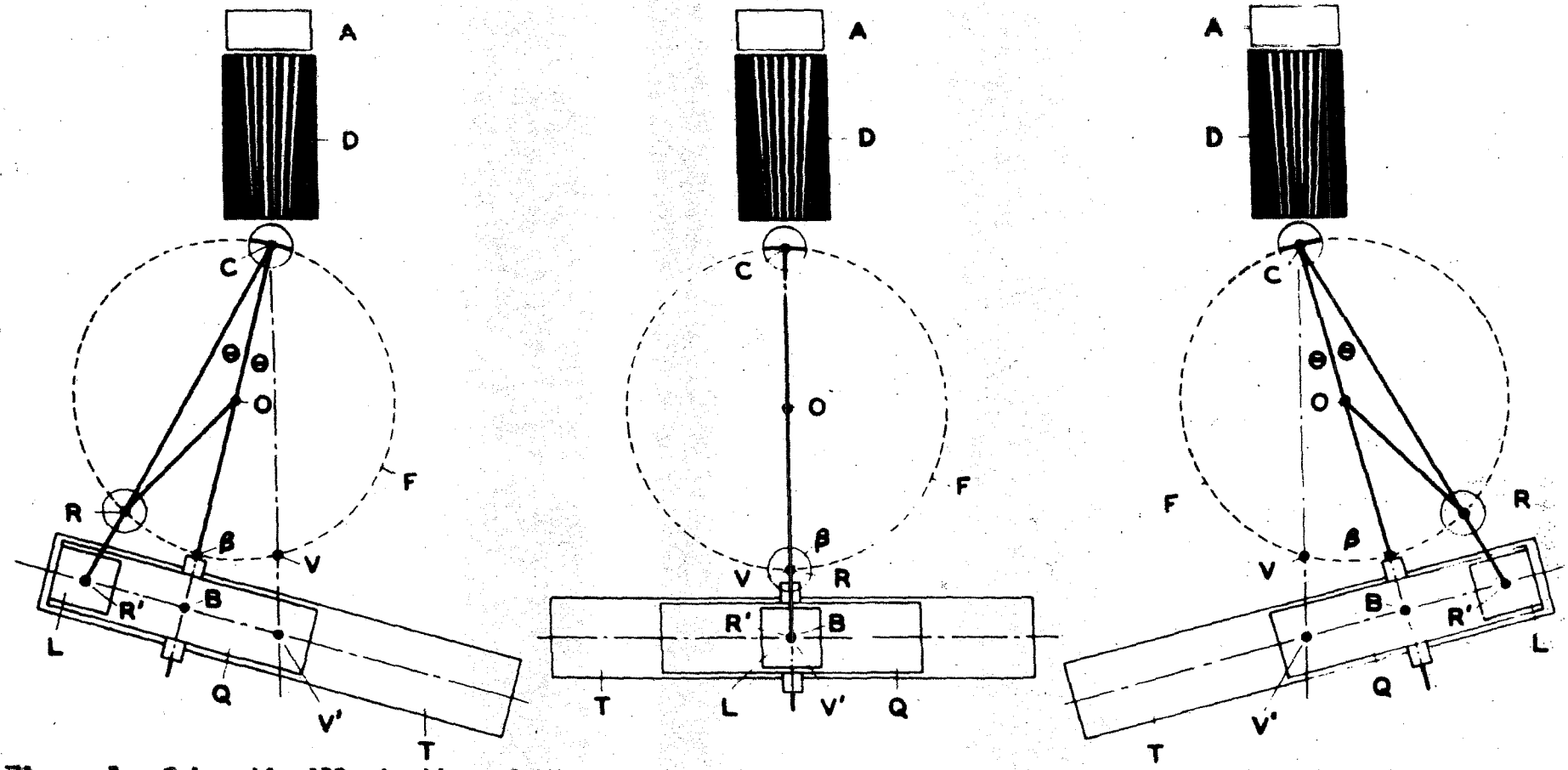

Figure 1. Schematic illustration of the geometry of the gamma-ray spectrometer. The view at center shows the instrument at the zero wavelength position, while the views to left and right show different wavelength settings for reflections to left and to right of the atomic reflecting planes. The constant distances CR' and CV' are made rigorously equal. Displacements of the carriages, L and Q, effected by means of precision screws, are proportional to the sine of the Bragg angle, and, hence, proportional to wavelengths. The drawing is not to scale. The aperture of the crystal at C and the width of the collimator are exaggerated.

very closely to Siegbahn x units, he can readily set the instrument to any desired wavelength. In practice, wavelength determinations are made by scanning the line profile as it is reflected on both sides of the zero wavelength position. The total difference in $\sin\theta$ between these two positions is therefore proportional to 2λ; thus wavelength determinations are made without reference to a zero wavelength position.

In this instrument the width of the spectral "window" as measured in wavelength units is approximately constant. The principal sources of line broadening, which determine the width of the instrument "window," are the aberrations from perfect focusing of the bent quartz crystal, its mosaic imperfections, its intrinsic diffraction pattern width and the geometrical breadth of the source on the focal circle. The full-width at half-maximum, $\Delta\lambda$, of this window profile is 0.28 xu for sources having a breadth of 0.008". Since the gamma rays measured with the instrument almost always have a natural line width which is very small compared with this value, the composite line width of a gamma ray is the same as the instrument window width. This is not true for x rays. A discussion of the effect of the natural line width of x rays is found in App. IV.

The relative energy resolution, $\Delta E/E$, of the instrument is equal to $E\Delta\lambda/K$ where $\Delta\lambda$ is, as has been said, approximately constant and k is the conversion factor from energy to wavelength. The value of k used was 12372.44 kev xu as given by Cohen, DuMond, Layton, and Rollett (16). Using the value of 0.28 xu for $\Delta\lambda$, the energy resolution is seen to be

$$\Delta E/E = 2.3 \times 10^{-5}\ E/1\ \text{kev} \quad . \qquad (2).$$

As an example, for an energy of 100 kev, the resolution is 0.23%. Fig. 2 shows a "bird's eye view" of the Hf^{180m} spectrum, as recorded using the spectrometer, illustrating the excellent resolution of the

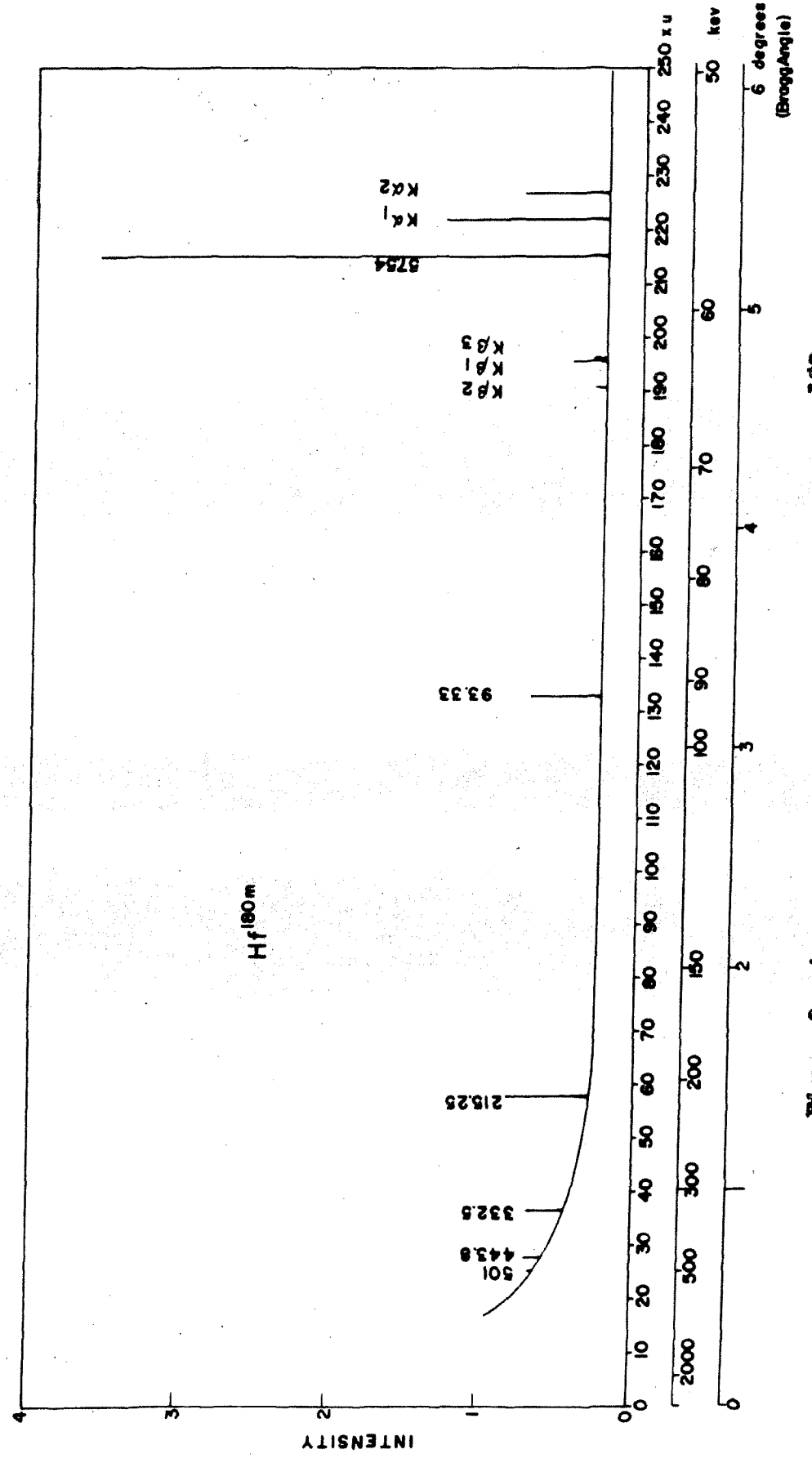

Figure 2. A sweep run of the gamma-ray spectrum of Hf^{180m} using the curved crystal spectrometer. The high resolution of the spectrometer is illustrated by the narrow width of the lines.

instrument.

The uncertainty in the determination of the energy of a strong line was taken to be 1/20 of the full-width while for a very weak line, 1/3 of the full-width was used. Applying the Ritz combination principle, the consistency of gamma-ray energy relations indicates that this estimate of error is very conservative. It is felt that the given error figures correspond to at least a 90% confidence level and hence represent about 1.5 standard deviation.

As one of the purposes of this study was to calibrate the spectrometer for gamma-ray intensity measurements, a discussion of the manner in which these measurements were made will be left to Part III.

Because the gamma-ray spectrometer played such a vital role in the experiments of this study, the alignment of the instrument was thoroughly checked and adjustments were made where necessary.

First a "Hartmann" test was performed to find the correct focal point of the crystal. Successive portions of the curved-crystal were blocked out and wavelength determinations made of a strong spectral line. A plot showing the ray path for each portion of the crystal indicated the radius of a focal circle where maximum resolution was to be found. The line used was the W $K\alpha_1$ x ray. Seven areas of the crystal were used on both sides of the zero wavelength position of the spectrometer. Fig. 3 shows the results of the test for reflection on one side of the planes which indicated that the focus was 0.74 cm from the focal setting where the tests were made. The test with reflection from the other side of the planes indicated a deviation of 0.85 cm. The source was therefore adjusted 0.80 cm closer to the crystal. This adjustment was made in such a manner as to insure having equal distances from the center of the focal circle O (as shown in Fig. 1) to the source R and

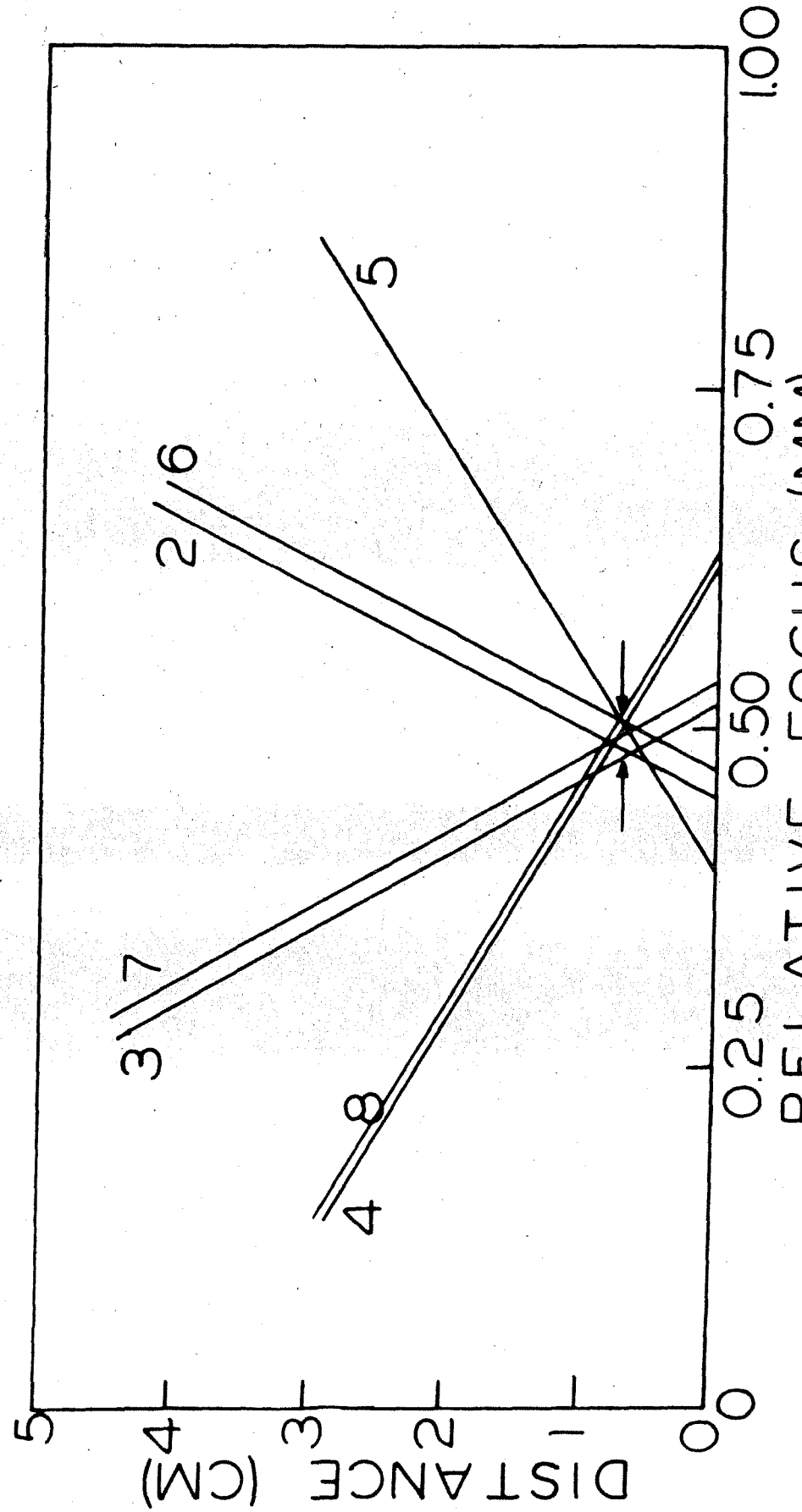

Figure 3. "Hartmann" test for finding the position of the focus (the circle of least confusion) of the gamma-ray spectrometer. The paths of the gamma rays coming from different regions of the quartz crystal are shown. The horizontal scale has been increased by a factor of 100 over the vertical.

crystal C. The correct positions were determined and careful adjustments made using an inside micrometer.* It is interesting to note that before these adjustments were made, an intensity difference of about 10% existed between lines measured on the two sides of the zero position of the spectrometer. After the alignment was made, however, these intensities became equal to within a few percent.

The collimator was then aligned so that it transmitted the selectively reflected gamma-ray beam with maximum intensity. It was noticed that this adjustment was surprisingly sensitive if one desires to take advantage of the last 10% of intensity that can be obtained. The collimator position does not limit the resolution of the spectrometer but governs to what energy the instrument can be used without interference from the direct beam.

With these adjustments made, the spectrometer was ready for an extensive intensity calibration which will be discussed in Part III.

B. Magnetic Beta-ray Spectrometers

The magnetic beta-ray spectrometers have been previously described in the literature (17) (18). The homogeneous-field spectrometer which is used for measurements of electrons with energies greater than 25 kev is a ring focusing device having high luminosity. The magnetic field is controlled using proton resonance heads, the measured quantity being the resonance frequency. The detector is a Geiger-Müller counter having a mica window of thickness 0.9 mg/cm^2. Since the beta particles are incident at 45° thereon, this is equivalent to a 1.4 mg/cm^2 window. Source preparation will be described later.

---

* The supervision and active assistance of Mr. Herbert E. Henrikson during this portion of the instrument alignment is gratefully acknowledged.

Beta spectra are studied by measuring the counting rate as a function of the magnetic rigidity, $B\rho$. This may be done either by using an automatic field scanning drive and a counting-rate meter with the counting rate being recorded on a strip chart recorder, or by using manual operation and a scaler to record the individual counts ("point by point" method). The momentum resolution of the spectrometer depends upon the size of the source and the settings of the spectrometer diaphrams. Sources were of two sizes. With the spectrometer adjusted to give "optimum match" of resolution and intensity the 3-mm diameter sources gave 0.7% momentum resolution while 1-mm sources gave 0.3% resolution.

The 180° beta-ray spectrometer was used to measure beta rays having energies between 2 kev and 120 kev. The current providing the nearly homogeneous magnetic field was controlled using a rotating electromechanical device and an electronic servo system. The detector for this spectrometer was a Geiger-Muller counter having a formvar window. Windows were made by a standard process (19) and varied in thickness from 10 $\mu g/cm^2$ to 30 $\mu g/cm^2$. The operation of this spectrometer was also either automatic or manual with the counting rate being recorded in the same manner as with the ring-focusing spectrometer. The "optimum match" momentum resolution for the 1.5 mm x 2.5 cm sources used was about 1%.

The observed counting rate is proportional to the number of electrons in the range of momenta between magnetic rigidities $B\rho$ and $B\rho + \Delta(B\rho)$. Since in this instrument $\Delta(B\rho)/(B\rho)$ is essentially constant, and hence $\Delta(B\rho)$ varies proportional to $(B\rho)$, it is necessary to divide the integrated number of counts in the area of each line profile by the corresponding $B\rho$ of that line in order to obtain numbers proportional to

the relative intensities of the different lines.

The corrections to the relative intensities are due to counter dead-time losses and to electron absorption in the counter windows. Dead-time corrections were made wherever the counting rate was sufficient to necessitate this. With the ring-focusing spectrometer, window-loss corrections were applied from curves given by Slätis (19) for mica windows. These curves give the correction factor to the observed electron intensity as a function of the energy of the electron. In the 180° spectrometer and for most lines in the ring-focusing spectrometer, the electron absorption was negligible.

C. Sources

All of the radioactive sources used in this study were produced by neutron capture. Generally, the materials to be irradiated with thermal neutrons were enriched in the isotope of interest, abundances varying from 40% to 95%. These separated isotopes were purchased from the Stable Isotope Division of the Oak Ridge National Laboratory. The neutron flux in which the material was placed varied from $10^{14}/cm^2$ sec to $8 \times 10^{14}/cm^2$ sec. With the high neutron flux, in addition to the high enrichments which were generally available, sources usually had an initial specific activity of the order of 500 mc/mg.

Transportation of the materials from the pile at Arco, Idaho, to the laboratory in Pasadena was generally accomplished by air because of the short half-lives of most of the sources studied.

Usually the source material for the curved-crystal spectrometer was enclosed in a fused quartz capillary tube of internal diameter near 0.009", external diameter near 0.050" and height 1". The ends of the capillary tube containing the material were fused together thus forming

a completely enclosed "line" source for the spectrometer. These were ready for immediate insertion into the instrument.

The preparation of sources for the beta spectrometers was accomplished by vacuum evaporation of the activated material onto a suitable backing. Backings used depended upon source material, evaporation temperature, and whether or not back scattering was important. Generally, aluminized mica or aluminum foil was used for backings. If the evaporation was made onto mica or aluminum foil, a circular source was punched out for the ring focusing spectrometer and a narrow rectangular source was cut out for the 180° spectrometer. These sources were glued to the spectrometer source holder with Duco Cement.

A description of the individual sources used in this study follows:

Hf^{180m}

Hf^{180m} sources were produced by neutron irradiation of HfO_2 with the hafnium enriched in the isotope 179. Table I gives the isotopic abundances for the two enrichments used. A contaminant activity due to radioactive Hf^{181}, produced by neutron capture of Hf^{180}, was minimized by the higher enrichment sources which became available during the course of the experiment. These sources increased the 179 to 180 isotopic abundance ratio from 1 to 8 thus decreasing the contamination activity correspondingly.

Sources were irradiated for about six hours in a neutron flux of approximately $2 \times 10^{14}/cm^2$ sec. Since the half-life of Hf^{180m} is 5.5 hours, longer irradiations were avoided to keep from increasing the percentage of the total activity contributed by the 41-day Hf^{181}. After removal of the sources from the pile, they were rushed to the laboratory

TABLE I. Hf isotopic abundances of the present enriched sources

Isotope	Abundance %		
	Natural[a]	Enrichment 1	Enrichment 2
174	0.16	trace only	<0.1
176	5.21	0.13	<0.1
177	18.56	1.17	1.2
178	27.1	4.89	4.6
179	13.75	47.55	83.6
180	35.22	46.27	10.0

a. From Strominger et al. (20)

in Pasadena.*

The vacuum evaporation of the beta sources was accomplished by placing the radioactive material in a recess in a tungsten ribbon filament. Very high temperatures, near 3200° C, were necessarily used. The evaporation was made directly onto the end of the aluminum source holder for the ring-focusing spectrometer and onto a pre-cut aluminum foil strip for the 180° spectrometer.

Se^{75}

The material used to produce the beta-active Se^{75} sources was enriched Se^{74} in the chemical form SeO_2. The abundance of the isotope in the enriched source was 12.3%. The internal diameter of the gamma-ray sources was approximately 0.008". The sources were irradiated in a neutron flux of approximately $4 \times 10^{14}/cm^2$ sec for 15 days.

The source backing for each of the beta-spectrometer sources was aluminized mica. The sizes of the sources used corresponded to 0.7% and 1% momentum resolution for the ring-focusing spectrometer and the 180° spectrometer respectively.

W^{187}

The sources were prepared by neutron irradiation of enriched W^{186} in the form WO_3. The abundance of the isotope in the enriched source was 97.9%. The neutron flux was approximately $2 \times 10^{14}/cm^2$ sec and the

---

* The time lapse between removal of the sources from the pile at Arco, Idaho, and their insertion into the instrument in Pasadena was generally about 13 hours. Effective measurements could then be made for about another 13 hours (two to three half-lives). Because of this short period during which the source could be studied many irradiations were necessary.

I am indebted to Messrs. J. L. Walker and R. R. O'Connor of Phillips Petroleum Company and the staff at the Materials Testing Reactor for the efficient handling of the irradiations and shipments and to Mr. A. Hicks of Caltech whose dependability and effective driving saved precious hours.

irradiation time was five days.

In addition to the quartz capillary gamma-ray sources with internal diameter of 0.009", an additional "extended" gamma-ray source was used. The extended source holder was made from very pure aluminum and had internal dimensions 0.010" x 0.250" x 1". An aluminum cap was welded to the holder, sealing it off. The thickness of the window presented to the gamma-ray beam was 0.010". This source holder was filled with about 100 mg of WO_3. The extended source was prepared in order that very weak high energy gamma-ray transitions in Re^{187} could be studied. With this source, intensities of gamma rays whose energies were above about 200 kev were increased considerably. For gamma rays of lower energies, self absorption through the 0.250" depth of the source caused the radiation to be absorbed out. Since only one rectangular cross section of the extended source could be placed in the focal position of the spectrometer, there was a line broadening of approximately 35% when using the extended source.

Beta sources were prepared by vacuum evaporation onto aluminized mica. The ring-focusing spectrometer was operated at 0.7 and 0.3% momentum resolution while the 180° spectrometer was operated at 1% momentum resolution.

Ta^{182} and Ta^{183} Sources

The source for the gamma spectrometer was prepared by obtaining a very pure tantalum wire whose diameter was 0.010" and length was 1.2" and by inserting it into a quartz capillary tube with an internal diameter small enough to assure a tight fit. The capillary tube provided rigidity sufficient to insure against the wire bending. Ta^{181}, the isotope from which $Ta^{182,183}$ are formed by neutron capture, was

virtually the only isotope contained in the source as its natural abundance is almost 100%, and the chemical purity was high.

The source was irradiated for approximately 30 days at a neutron flux of approximately $4 \times 10^{14}/cm^2$ sec. The 112-day Ta^{182} was produced by neutron capture and the 5-day Ta^{183} by double capture. The double capture activity was considerable because of the fairly short half-life of the 183 isotope and especially because of the large cross section for neutron capture of Ta^{182}, which is 13000 barns.

As the relative intensities of the gamma rays were the only quantities to be determined with these isotopes, no beta sources were made.

Part III

CURVED-CRYSTAL SPECTROMETER INTENSITY CALIBRATION

A. GENERAL

As previously mentioned, there has been considerable question as to the accuracy of the gamma-ray intensities measured using the curved-crystal spectrometer. For this reason a new intensity calibration was performed.

The heights of the gamma-ray lines as registered in the spectrometer can be used directly as a measure for their intensities instead of using their areas because the instrument window is constant on a wavelength scale.* Intensity measurements are made, therefore, by positioning the spectrometer at the peak of the line and determing the counting rate. Then the background counting rate is determined on each side of the line.

The number of counts per unit time at a particular spectrometer setting is determined by detecting the photons with a NaI (Tl) crystal. A photomultiplier tube collects the light and the resulting electrical pulses are amplified and fed into a 100-channel pulse-height analyzer to be analyzed and recorded.

Energy dependent corrections to the counting rate fall into three groups:

First, corrections due to absorption. These include self absorption in the source, absorption in the source container, in the air path, in the bent quartz crystal, and in the aluminum window of the NaI(Tl) crystal container. Second, corrections for the photopeak efficiency of

---

* This only applies when the natural line width is small as compared with the instrument window width, as is the case for most gamma rays but not for x rays. The subject is discussed in detail in App. IV.

the detector. Third, corrections due to the energy dependent reflection properties of the bent quartz crystal. All of these corrections could be made from previously existing data except for the reflectivity correction.

Absorption Corrections

The absorption corrections were made using the absorption coefficients of Grodstein (21) and McGinnies (22). All absorption corrections are straightforward with the possible exception of the self absorption in the source. In making the latter correction, the source geometry is important. Two source shapes were used. The first was a right circular cylinder. The second was an extended source of rectangular cross section. The calculation of the source absorption correction to be applied in the case of the rectangular geometry was straightforward. However, for the cylindrical sources (usually called "line" sources) the integral involved in making this correction did not have a simple analytical solution. For this reason it was expanded in a power series and integrated term by term. The result follows:

$$I/I_o = 1 - 0.849\,\omega + 0.500\,\omega^2 - 0.226\,\omega^3 + 0.083\,\omega^4 - 0.032\,\omega^5 + 0.0111\,\omega^6 - 0.00163\,\omega^7. \qquad (3)$$

I is the beam intensity as it emerges from the surface of the source, I_o is the intensity if absorption were not present, ρ is the density of the absorbing material, μ is the mass absorption coefficient, a is the radius of the source, and $\omega = \mu\rho a$.

Detector Efficiency

The efficiency of the NaI(Tl) detector, which has dimensions 5" diameter x 3" deep, was calculated from a formula given by Berger and Doggett (23). The formula assumes a well collimated, narrow beam

incident upon the center of the crystal parallel to the cylindrical axis and neglects the escape of secondary radiation. This calculation is expected to be good for the present crystal as the diameter of the face is 5" whereas the beam is a square about 3" on a side. The beam is well collimated and the size of the crystal assures very good absorption of the incident photons and little escape of secondary radiation in the form of bremsstrahlung or Compton scattered quanta, for radiation whose energy is within the practical limits of the spectrometer for reliable intensity measurements (30 kev to about 600 kev). Fig. 4 shows a plot of the efficiency of the present crystal as a function of energy. The "photo efficiency" is actually a combination of photopeak plus escape peak efficiencies. It is fortunate that the efficiency of the crystal is 100% to about 200 kev and that the correction over a considerable part of the useful range of the spectrometer is small.

The escape peak correction which is important for energies under 100 kev has been empirically determined by diffracting monochromatic beams of gamma rays of known energies with the spectrometer. The spectrum resulting from the detection of these beams by the NaI(Tl) detector was then analyzed to determine the ratio of the escape peak intensity to the photopeak intensity. By using several strong gamma rays, this correction was determined as a function of energy. The resulting points are shown in Fig. 5. The correction is somewhat less than that given by Wapstra et al. (24). Indeed, it appears to be somewhat less than that calculated by Axel for a "very good geometry" crystal (25).

Fig. 6 shows the combined effect of all those instrumental corrections to the observed line intensities (for absorption and counter efficiency) which are independent (1) of source geometry and material and (2) independent of the bent quartz-crystal reflectivity. The

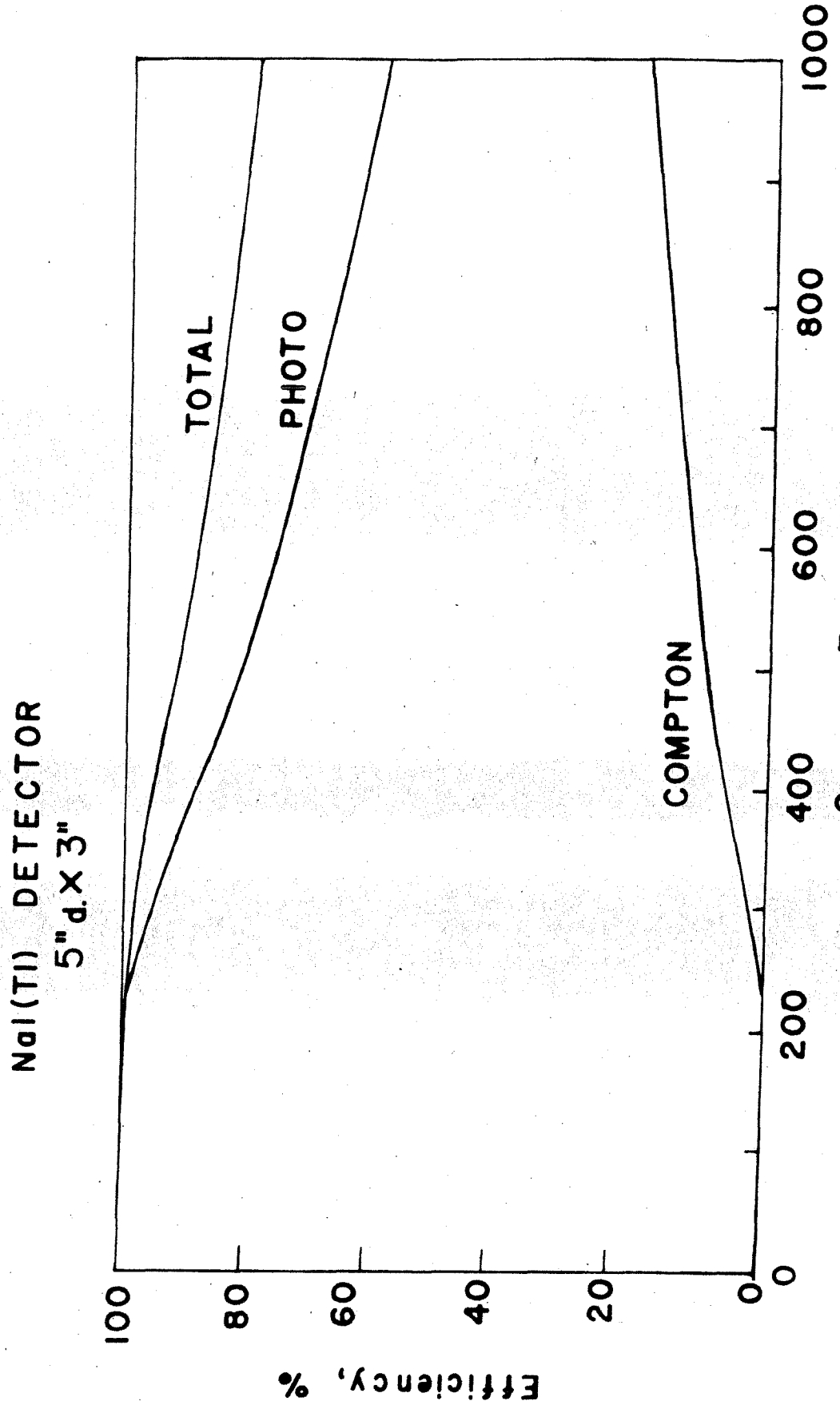

Figure 4. The efficiency of the 5" diameter by 3" NaI(Tl) detector used in the curved-crystal gamma-ray spectrometer, calculated using a formula by Berger and Doggett (18). The "photo" efficiency actually includes the sum of the photopeak efficiency and the escape peak efficiency. The sum of the Compton efficiency and the "photo" efficiency equals the total efficiency.

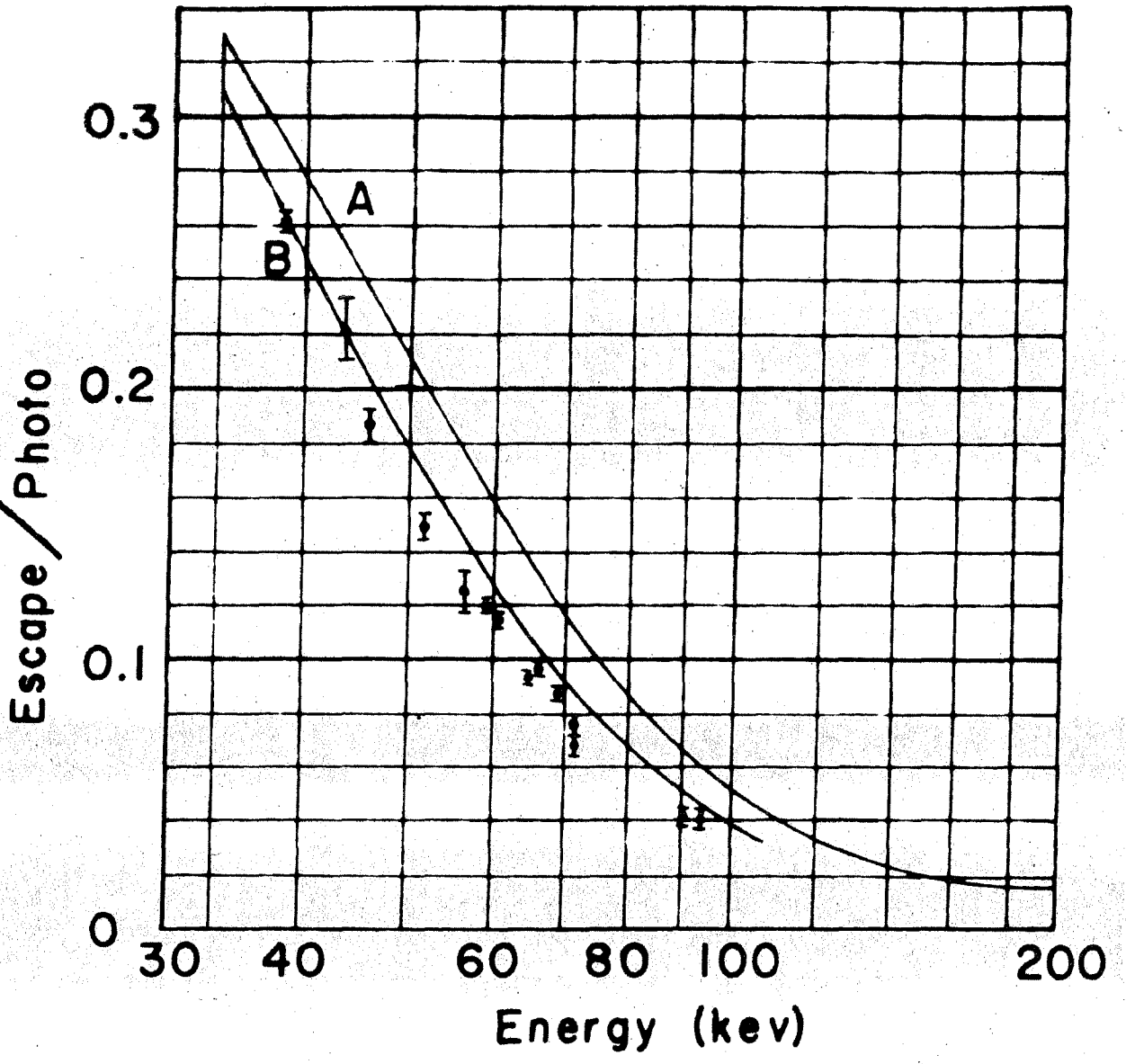

Figure 5. The ratio of the escape peak to photopeak intensity as a function of energy for the 5" diameter by 3" NaI(Tl) detector used with the curved-crystal gamma-ray spectrometer. The points are the empirical determinations of the ratio. Curve A is that given by Wapstra et al. (19). Curve B is the ratio given by Axel for a "very good geometry" crystal (20).

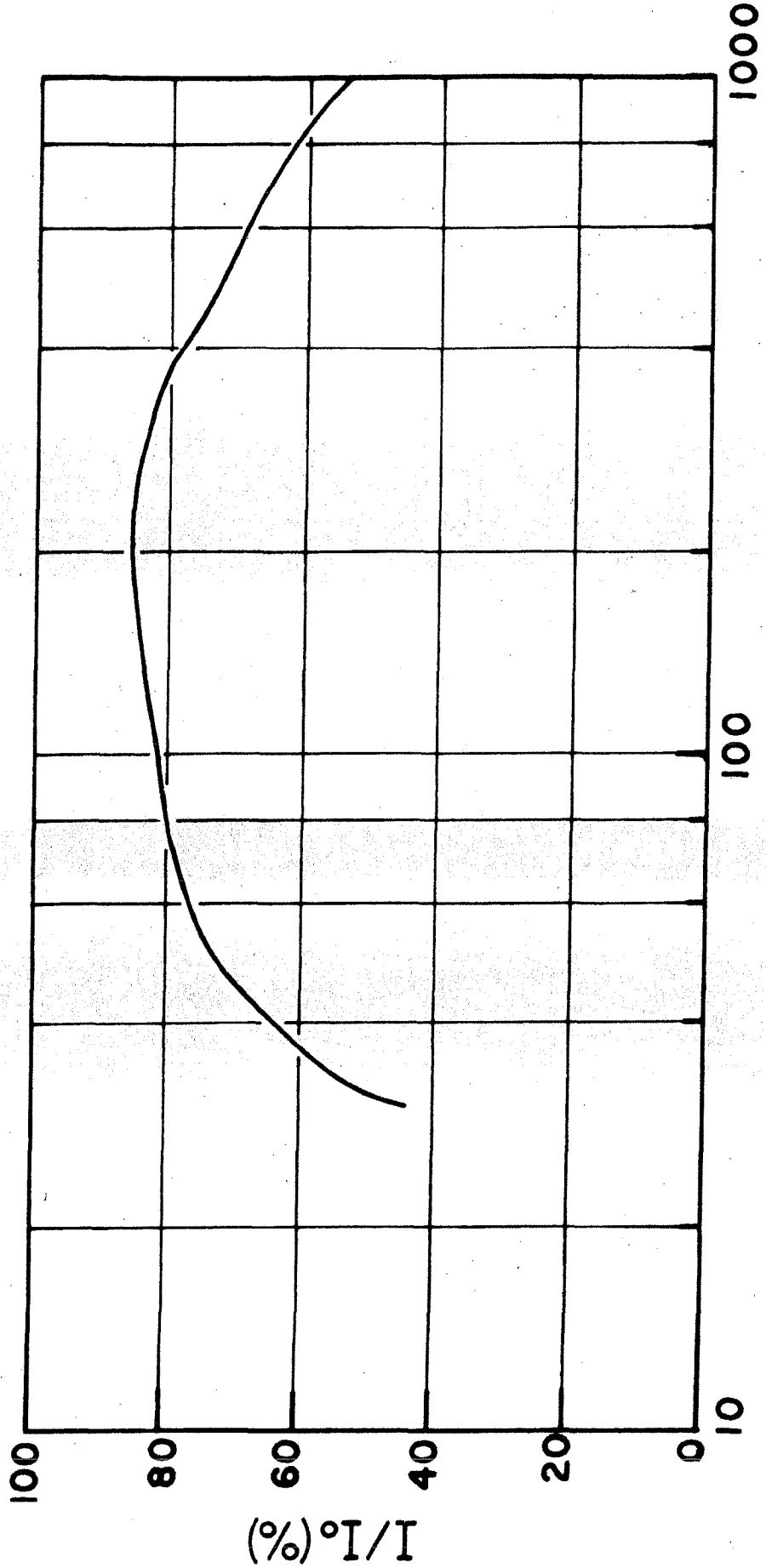

Figure 6. The combined effect of many corrections factors in the curved-crystal spectrometer which reduce the number of photons being detected. These factors include absorption in the air path, bent quartz crystal absorption, absorption in the aluminum window of the detector, and "photo" efficiency of the detector.

standard deviation to be attached to intensity corrections taken from the curve of Fig. 6 depends upon the energy difference of the gamma rays whose intensities are being compared, increasing with the disparity of their energies but in no case exceeding 1.5% for the range of energies shown in Fig. 6. More uncertain by far has been the correction due to the energy dependence of the reflectivity of the quartz crystal.

Curved-crystal Reflectivity

Lind, West, and DuMond (26) (27) have reported that an unstressed quartz crystal has a peak reflection coefficient* that varies more slowly than $1/E$ and approximately as $\lambda^{0.58}$. When the quartz is stressed, this relationship changes. They found that for a stressed crystal 1 mm thick, the dependence is near λ^2 or E^{-2}. Hatch (28) found that this dependence also seems to hold for a 2-mm thick crystal. He stated that it was closer to E^{-2} than to E^{-1} or E^{-3}. For two gamma rays whose energies differ by a factor of four, an uncertainty of 0.5 in the exponent gives a relative intensity uncertainty of a factor of two. It was apparent that a precise value must be found if the curved-crystal spectrometer was to fulfill its capabilities.

Possible Calibration Methods

There are two general approaches to the problem of intensity calibration. The first (which shall be called a "unified calibration") is to find an empirical curve relating uncorrected relative intensities to actual relative intensities in the source without recourse to the many individual corrections. The second ("individual correction calibration")

* The term "integrated reflection coefficient" has been used in the past. For the difference, refer to Appendix IV.

is to determine all of the known corrections individually and then compute the combined effect upon intensity measurements.

Because the major correction is that due to the reflection coefficient of the curved crystal, either approach should primarily determine this quantity because all other known corrections are secondary and calculable. A list of methods or experiments that, at least in principle, are capable of yielding information relevant to the calibration of the curved-crystal spectrometer follows:

1) Crystal reflectivity determination (Individual correction calibration).

a) By measuring gamma rays in the diffracted position and also in the direct beam (zero wavelength) position where the rays are not diffracted, the actual reflection coefficient as a function of energy may be determined. In this method all other corrections cancel out, for the amount of absorbing material through which the gamma rays travel is the same except for small differences in the air path. This was the method used by Hatch (28).

b) By using isotopes whose decay schemes contain a single strong gamma ray, the real ratio of the intensity of the gamma ray to the sum of the intensities of the K x rays may be determined, if the K-shell fluorescence yield, ω_k, and the K-conversion coefficient is known, by using the formula

$$I_{e_k}/I_\gamma = a_K \omega_k \, . \qquad (4)$$

By comparing the measured values with the calculated values, the intensith correction factor between these two energies can be determined.

2) Unified calibration.

a) By comparing the relative intensities measured using the curved-

crystal spectrometer with intensities measured with other instruments whose corrections are well known, the spectrometer may be calibrated.

b) The continuous x-ray spectrum might conceivably be used, for the intensity is reported to be linear with energy; thus one need but mount an x-ray tube in the source position and measure the intensities at various energies to determine the calibration. However, the shape of the continuous spectrum is insufficiently well verified. In addition, it is difficult to obtain sufficiently high voltages to calibrate the instrument over a useful range of energies.

c) By taking advantage of the over-determination which can be achieved with relative intensities when information about the populating and de-populating of excited nuclear levels is available, a calibration may be effected. This is called the "decay scheme method". It is discussed in detail in the next section.

One disadvantage of the individual correction approach is that one can never be completely certain that all corrections have been included. An over-all calibration of the instrument was felt to be the most satisfactory solution. In fact, however, the practicality of the experiment was a more important factor in determining the approach to the calibration problem. Two methods were decided upon, the method of comparing intensities with those measured with other instruments, and the decay scheme method (2a and 2c).

B. COMPARISON OF INTENSITIES MEASURED WITH OTHER INSTRUMENTS

Studies recently made of the decay scheme of Se^{75} offer gamma-ray intensity measurements which can be used to check the calibration of the curved-crystal spectrometer. Se^{75} decays by electron capture to As^{75}. In decaying to the ground state, the excited As^{75} nucleus emits

nine gamma rays with intensities large enough to be studied by the crystal diffraction method. These gamma rays range in energy from 66.05 kev to 400.7 kev, thus covering well the most useful range of the curved-crystal spectrometer.

Three other research groups have also measured the relative gamma-ray intensities, two of them by external conversion and one by sodium-iodide spectroscopy. Schardt and Welker (29) made important initial measurements of relative gamma-ray intensities by means of a sodium-iodide crystal detector. More recently, Grigorev et al. (30) have studied the gamma rays using external conversion, measuring the conversion electrons with a lens spectrometer. Metzger and Todd (31) have measured the relative intensities of five of the gamma rays by using external conversion. The relative intensities reported by these groups are given in Table II.

The values measured here, as corrected for crystal reflectivity by an exact E^{-2} law, are shown in column 6 of the table. From these data, the actual reflectivity correction was determined as follows: The mean of the values measured by other groups was found weighting the measurements according to the reported errors. The bent-crystal intensity uncorrected for crystal reflectivity was then divided by the mean of the other measurements to give values which then represented the curved-crystal reflectivity in relative units normalized to unity for the 264.62-kev line. When plotted on log-log paper, the reflectivity as a function of energy shows a very nice straight-line nature which indicates that the function does indeed follow an E^{-x} law where the exponent x is not itself a function of energy, as shown in Fig. 7.

To determine the best value of the exponent and its uncertainty, a least-squares adjustment was performed. The intensity when normalized

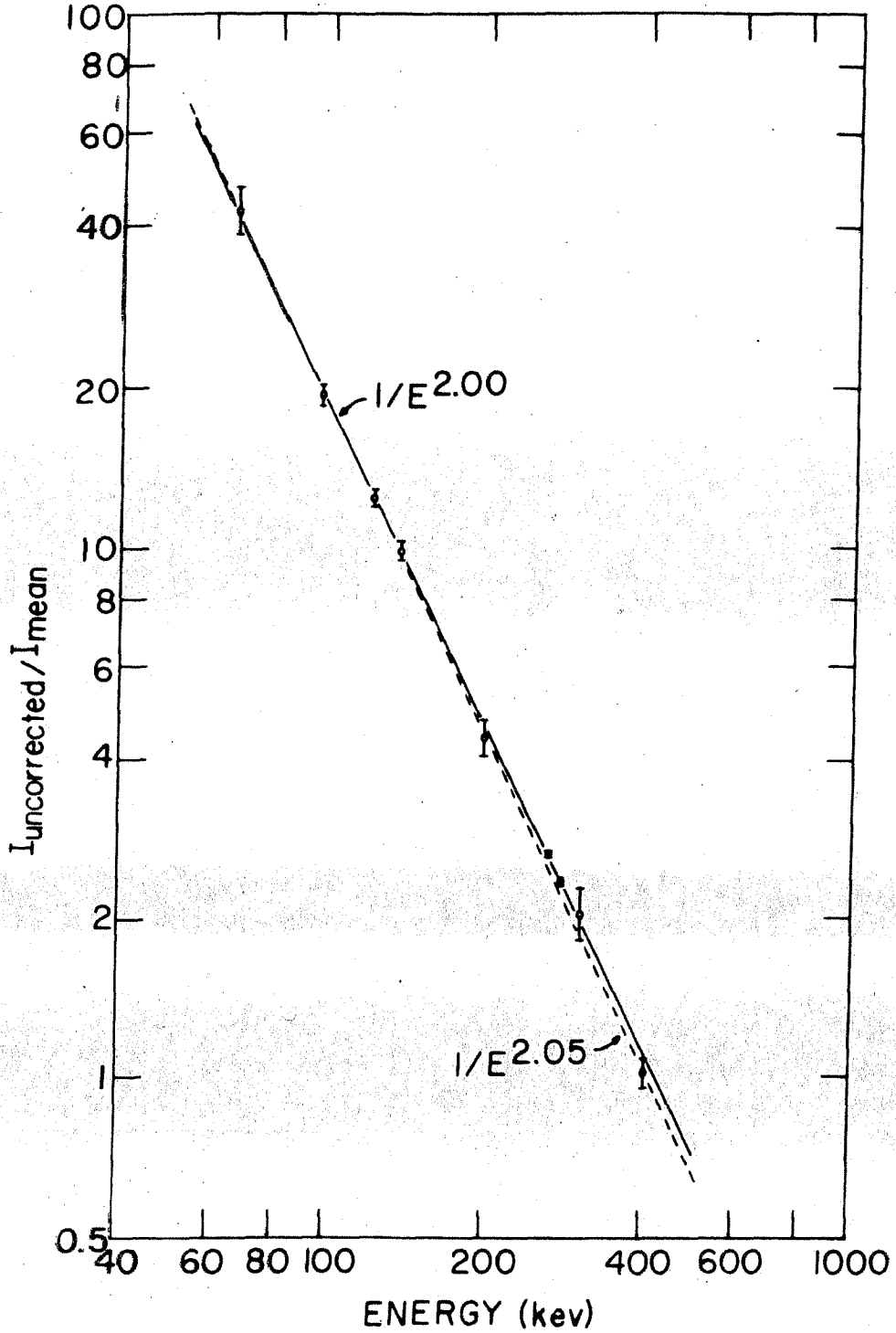

Figure 7. The determination of the quartz-crystal reflection coefficient. The gamma-ray lines in Se^{75} decay as measured with the curved-crystal spectrometer are compared with those measured by several other authors. $I_{uncorrected}$ is the intensity measured here uncorrected for reflection coefficient variation. I_{mean} is the mean value of the other investigators. A least squares adjustment indicated a $E^{-2.000\pm0.032}$ relationship.

Table II. As^{75} gamma-ray intensity data.

Gamma-ray energy, present measurement (kev)	Gamma-ray Intensity					
	With other instruments				With the curved-crystal spectrometer	
	Schardt and Welker (29)	Grigorev et al. (30)	Metzger and Todd (31)	Mean Value	Corrected with E^{-2000} a	Corrected with $E^{-1.987 \pm 0.022}$ b
66.05 ± 0.01	1.8±1	1.53±0.15		1.53±0.15	1.60±0.03	1.63±0.06
96.74 ± 0.01	6.6±1.5	5.5 ±0.3		5.6 ±0.3	5.50±0.09	5.57±0.18
121.12 ± 0.01	29 ±4	27.9 ±1.3		28.0 ±1.2	27.7 ±0.4	28.0 ±0.6
135.99 ± 0.02	94 ±12	96 ±5		95.6 ±4.6	94.7 ±1.0	95.5 ±1.8
198.60 ± 0.06	~3	2.6 ±0.2		2.6 ±0.2	2.4 ±0.1	2.4 ±0.1
264.62 ± 0.07	100	100	100	100	100	100
279.57 ± 0.08	45.7±4	41 ±2.5	47 ±1	46.2 ±0.9 42.2 ±2.1 c	42.2 ±0.6	42.2 ±0.6
304.0 ± 0.3	2.0±0.5	2.5 ±0.3	2.1±0.3	2.25±0.20	2.29±0.14	2.29±0.14
400.7 ± 0.2	24.8±2.5	22.3 ±2.3	19 ±2	21.6 ±1.3	19.6 ±0.6	19.5 ±0.6

a. These intensities were obtained assuming a curved-crystal reflectivity correction proportional to E^{-2000}. The errors do not include a reflectivity uncertainty.

b. These intensities were obtained in accordance with the present spectrometer intensity calibration which indicates a curved-crystal reflectivity proportional to $E^{-1.987 \pm 0.022}$.

c. This value is the mean of the values obtained by the first two groups. For a discussion of this see p. 34.

to a particular energy is

$$I/I_u = (E_o/E)^{2+x} \tag{5}$$

$$\text{or} \quad \log I/I_u = (2 + x) \log (E_o/E) \tag{6}$$

where E is the energy of the line, E_o is the reference energy (where the correction is equal to unity), and I_u and I are the uncorrected and corrected relative intensities respectively. The only parameter to fit to the input data is x, the correction to the exponent 2 in the reflectivity law. The quantity (2+x) is the slope of the adjusted line when plotted in log-log units.

By examining Table II, one can see that the agreement between the experimental data is, indeed, very good. There does, however, exist a discrepancy between the reported intensities of the 279.57-kev line. All other Se^{75} data indicate a crystal reflectivity relationship very close to E^{-2} as did also an instrument calibration (to be described presently) using Hf^{180m}. Assuming the E^{-2} law, the intensity of the 279.57-kev line relative to the 264.62-kev line could be measured with considerable accuracy with the resulting relative intensity 42.2 ± 0.6. The error is almost entirely due to counting statistics. As the energy difference is small, the uncertainties due to energy dependent corrections were negligible. The present value over-laps that of Grigorev et al. and also that of Schardt and Welker; however, it is about seven standard deviations from that of Metzger and Todd. Because of this great difference, the point was carefully remeasured until the total number of measurements on this line was four (the other lines were measured twice). The reproducibility was good, the highest value being 42.7 and the mean 42.2. The lines were entirely resolved and very strong. It was therefore felt that the value of Metzger and Todd was in error and, hence,

this value was not used. This did not, however, have a great effect on the output value of the exponent. The difference, if the value by Metzger and Todd had been used, would have amounted to less than 0.3%. The adjusted value of x was found to be 0.000 ± 0.032 giving an exponent in the reflectivity law of 2.000 ± 0.032 over the range $60 \text{ kev} \leq E \leq 400 \text{ kev}$. The quoted error is the standard deviation, σ_i, reflecting the accuracy of the original measurements, or internal error. The consistency of the data is good, for the standard deviation, σ_e, based on the spread of the observations (external error) is 0.024 giving $\sigma_e/\sigma_i = 0.75$.

C. DECAY SCHEME METHOD USING Hf^{180m}

To describe this method in a simple manner, a hypothetical decay scheme will be used. This is shown in Fig. 8. Level C is populated by beta decay from the parent nucleus. Level B and the ground state may, of course, also be populated. Measurements can be made with a gamma spectrometer of the relative intensities of the gamma rays $I(2)_\gamma/I(1)_\gamma$ and $I(3)_\gamma/I(1)_\gamma$, assuming the intensity calibration of the instrument is known. The quantities measured in the beta spectrometer are the relative conversion electron intensities $I(1)_{eL_I}/I(1)_{eK}$, $I(2)_{eK}/I(1)_{eK}$, etc.

For transition i, the conversion coefficient $\alpha(i)_\mu$ is defined as the ratio of the intensity of the electrons internally converted in the μ shell to the intensity of the gamma rays pertaining to that transition. Using only relative intensities, absolute conversion coefficients cannot be obtained without further information. When one absolute coefficient has been established, however, the others can be calculated from the measured relative beta- and gamma-ray intensities from the following relationship:

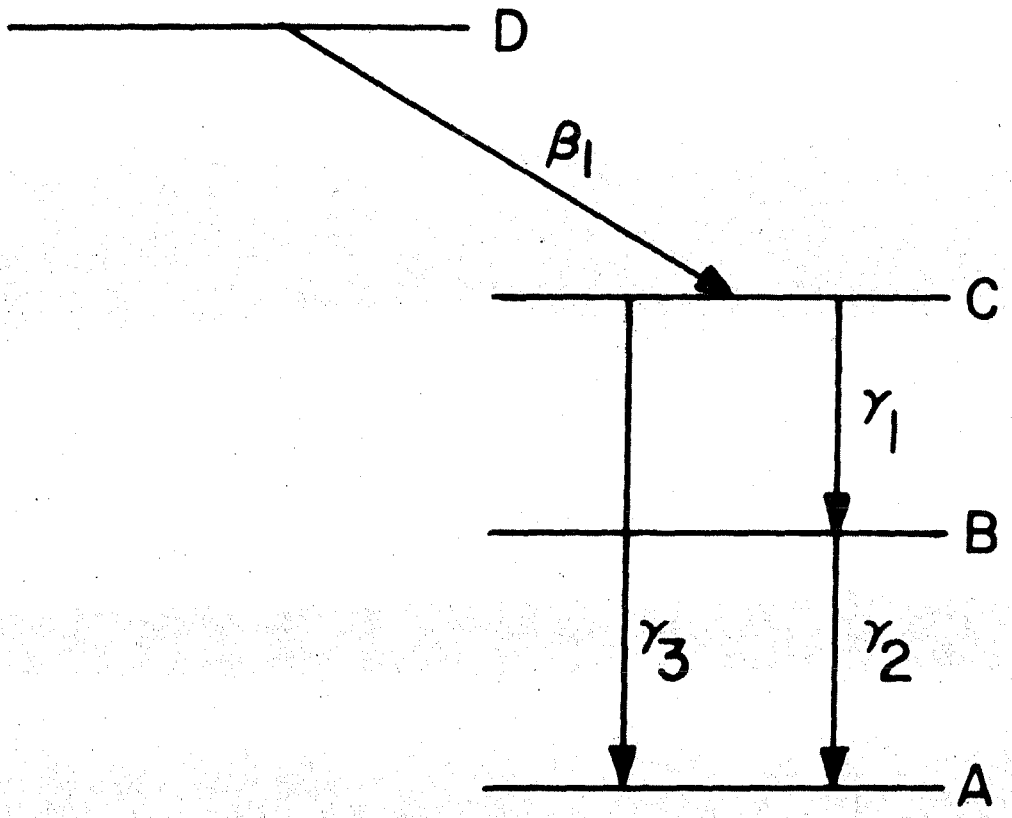

Figure 3. A hypothetical decay scheme to illustrate the decay scheme method.

$$\alpha(i)_{\mu} = \left[I(i)_{e_{\mu}} / I(1)_{e_K}\right] \cdot \left[I(1)_{\gamma} / I(i)_{\gamma}\right] \alpha(1)_K \qquad (7)$$

Now, the decay scheme can give relevant information by considering the populating and de-populating (feeding and bleeding) of levels. The decay fraction, which is the percentage of the total decay rate contributed by a particular transition, is proportional to $\left[1 + \alpha(i)_t\right] I(i)_{\gamma}$, where $\alpha(i)_t$ is the total conversion coefficient of the i^{th} transition. Referring to the hypothetical decay scheme, it is seen that equations can be set up in terms of the decay fractions expressing the fact that the feeding of level C equals the bleeding of C, and so forth. These equations relating the decay fractions shall be called "level equations." The number of independent equations that can be set up in this manner is equal to the number of intermediate states between the initial state, D, and the ground state, A. It is very difficult, however, to measure a beta-decay transition intensity; therefore, in practice, one cannot write an equation equating the feeding and bleeding of a level that is being fed by beta decay. In the example, the one equation that is useful is the equation written with respect to level B, if beta branching to that level does not occur,

$$\left[1 + \alpha(1)_t\right] I(1)_{\gamma} = \left[1 + \alpha(2)_t\right] I(2)_{\gamma}. \qquad (8)$$

Using Eq. (7) to eliminate $\alpha(2)_t$ and solving for $\alpha(1)_t$,

$$\alpha(1)_t = \left[\left(I(2)_{\gamma} / I(1)_{\gamma}\right) - 1\right] \cdot \left[1 - I(2)_{e_t} / I(1)_{e_t}\right]^{-1} \qquad (9)$$

Thus an expression has been obtained for $\alpha(1)_t$ in terms of the measured relative gamma-ray intensities and the relative total electron intensities. This expression can be used to find the absolute conversion coefficient of transition 1 which could then be used to normalize in an absolute manner all of the relative conversion coefficients in

the source.* If, however, the absolute conversion coefficients have been determined in some other manner, then Eq. (9) over-determines the system. This over-determination can, for instance, be used to obtain corrections to the relative gamma-ray intensities if the latter are not known with precision.

In a more complex decay scheme, equations giving a greater over-determination can be set up if there is no beta feeding of the levels or other quantities that cannot be experimentally determined. Thus, with a decay scheme such as Hf^{180m}, which has four intermediate levels, one can determine absolute conversion coefficients and still have a thrice over-determined system. The absolute coefficients were obtained and the over-determination was used to calibrate the gamma-ray spectrometer for intensity measurements.

Referring to Fig. 9, it is seen that, in the decay of Hf^{180m}, there are very few gamma rays between levels, the only cross-over being that of the 501-kev transition from the 9- state to the 6+ state. In addition, there is no beta activity at all which allows all intermediate level equations to be used and, in addition, reduces the beta spectrometer background considerably.

Spectrometer Calibration

To apply the decay scheme method to Hf^{180m}, measurements were made of the relative gamma-ray intensities using the curved-crystal

---

* It is interesting to note that when Eq. (9) is applied to cases where one of the gamma-rays is absent and the transition proceeds by electron conversion, such as in the case of the M4 transitions in the Te series of isomeric transitions, the expression simplifies to the point that the absolute coefficient of the M1 transition following the M4 transition can be measured using beta spectrometer relative intensities alone. $\alpha(2)_t = \left[\left(I(1)_{et} / I(2)_{et}\right) - 1\right]^{-1}$ where transition 1 is completely converted.

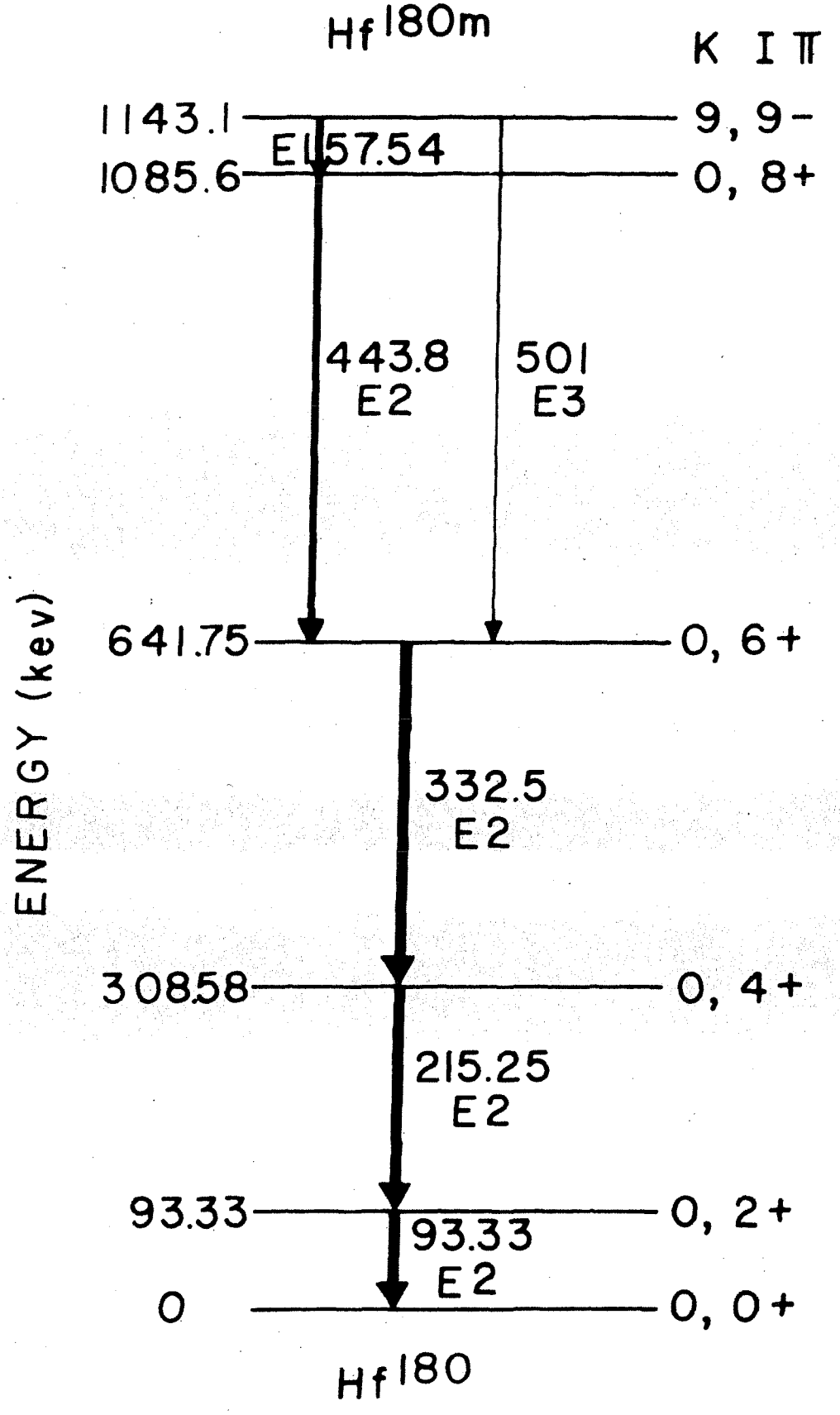

Figure 9. The decay scheme of Hf^{180m}.

spectrometer; relative conversion electron intensities were measured using the two beta-ray spectrometers. Gamma-ray intensities corrected for an E^{-2} reflection energy dependence are shown in Table III. Statistical uncertainty was of the order of 1% for most of the lines. The intensity of the 501.0-kev line was very inaccurately determined, however, as the line was very weak.

The ring focusing spectrometer which was used to measure conversion lines including the 93.33-kev L lines and all lines with higher energy was operated at 0.7% momentum resolution. The counting rate for a typical line was of the order of 700 counts per minute at the peak of the line. Total counts in the peak position were usually about 2000. The 180° spectrometer was used to measure the intensities of conversion lines including the 93.33-kev M lines and all lines with lower energy and was operated at 1% momentum resolution. Counting rates were similar to those found using the ring-focusing spectrometer. Fig. 10 and Fig. 11 show typical runs made with the 180° spectrometer. Although the beta spectrometers are equipped for automatic operation, all of the intensity runs were made manually. The time spent on each line varied from half an hour to two hours depending upon the relative line strength and state of decay of the source.

Table III gives the total of the intensities of the conversion lines for each transition. In the cases of the 215.25-, 332.5-, and 501.0-kev transitions, all of the conversion lines were not measured. The total electron intensities for these lines were found by adding to the sum of the experimental conversion line intensities a fraction to account for the unmeasured lines. The fraction was an "educated guess" based upon the general manner in which conversion coefficients vary between electron shells. A very large error was assigned to

Table III. Hf^{180} transition data used in the calibration of the curved-crystal spectrometer and in obtaining absolute conversion coefficients.

Gamma-ray energy (kev)	Total conversion electron intensity (relative units)[c,d]	Gamma-ray intensity[a] corrected with $E^{-2.000}$	Gamma-ray intensity[b] corrected with $E^{-1.987 \pm 0.022}$
57.54 ± 0.01	0.378 ± 0.013	289 ± 6	291 ± 7
93.33 ± 0.02	0.956 ± 0.023	100 ± 2	100 ± 2
215.25 ± 0.13	0.221 ± 0.010	506 ± 10	500 ± 14
332.5 ± 0.3	0.0634 ± 0.0025	577 ± 17	567 ± 24
443.8 ± 0.6	0.0227 ± 0.0012	502 ± 20	491 ± 26
501.0 ± 0.6[e]	0.0104 ± 0.0011	-	(102 ± 31)[f]

a. These intensities were obtained assuming a curved-crystal reflectivity correction proportional to $E^{-2.000}$. The errors do not include the reflectivity uncertainty.

b. These intensities were obtained in accordance with the present spectrometer intensity calibration which indicates a curved-crystal reflectivity proportional to $E^{-1.987 \pm 0.022}$.

c. The electron intensities should be multiplied by 5.38 to put them on the same scale as the gamma-ray intensities.

d. This includes the total of all subshell conversion electron intensities for each transition. For the 215.25-, 332.5-, and 501.0-kev transitions, all of the subshell lines were not measured and a correction was applied to account for the unmeasured lines. This is discussed on page 40.

e. The energy of this crossover transition was determined from the sum of the 57.54-kev and 443.8-kev cascade gamma rays.

f. This value was not measured directly but was deduced from the feeding and bleeding of levels as discussed on page 46.

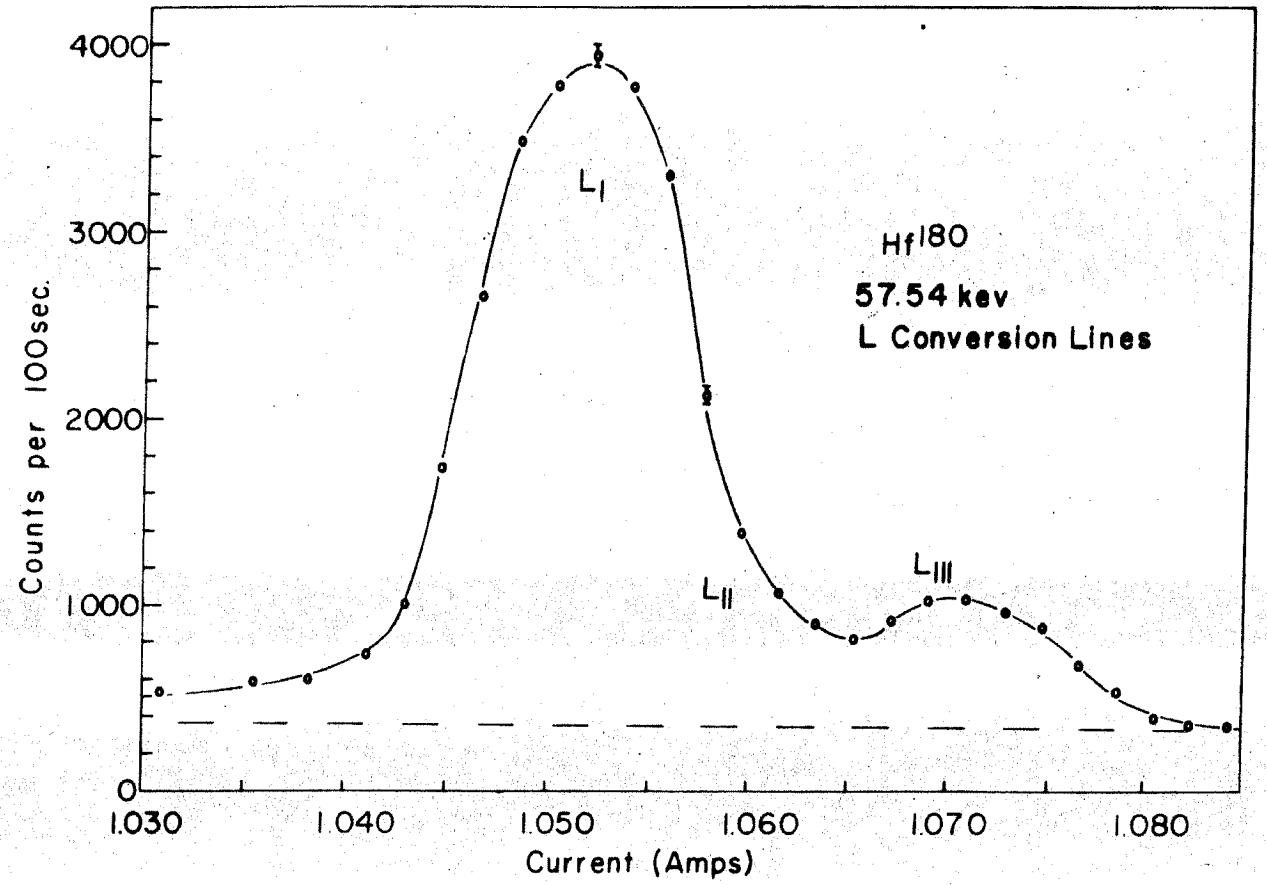

Figure 10. L-conversion electron lines of the 57.54-kev transition in Hf^{180m} as measured with the semi-circular spectrometer.

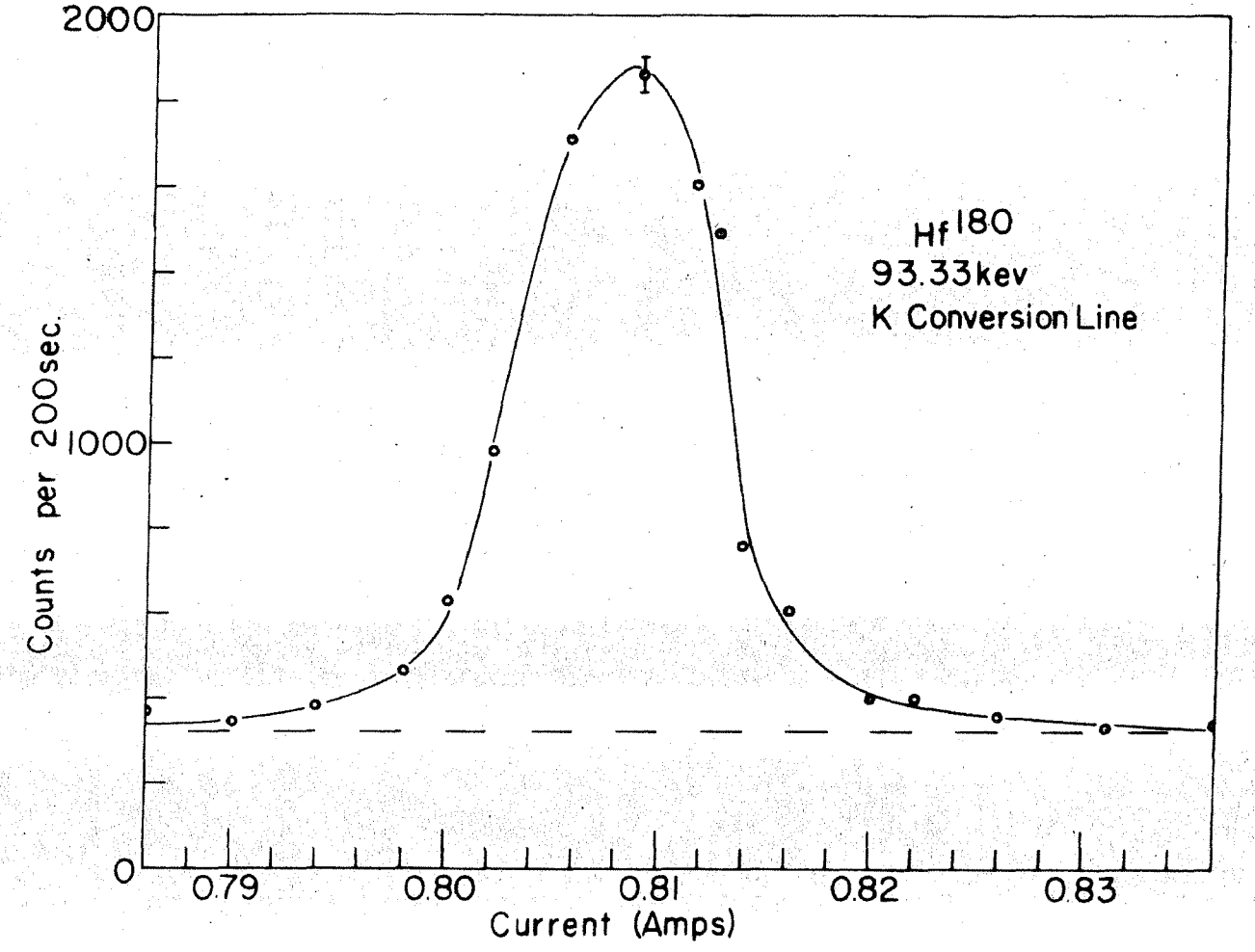

Figure 11. K-conversion line of the 93.33-kev transition in Hf^{180} as measured with the semi-circular spectrometer.

this fraction, amounting to 30% or more. Except in the case of the 501.0-kev line, this had little effect upon the uncertainty of the total conversion line intensity for the transition because of the small value of the fraction. The total conversion-electron intensity was measured directly for the 57.54-, 93.33-, and 443.5-kev lines.

Using the measurements of relative intensities, information from the decay scheme was invoked to aid in the gamma-spectrometer calibration and in obtaining absolute conversion coefficients. Referring to the decay scheme in Fig. 9, it is seen that level equations may be written for the 2+, 4+, 6+, and 8+ levels. These four equations may be written in the following form: (10)

$$\left[\left(I(216)_e / I(93)_e\right) - 1\right] \alpha_{93} = \left[1 - \left(I(216)_\gamma / I(93)_\gamma\right)\right] \qquad 2+$$

$$\left[\left(I(332)_e / I(93)_e\right) - 1\right] \alpha_{93} = \left[1 - \left(I(332)_\gamma / I(93)_\gamma\right)\right] \qquad 4+$$

$$\left[\left(I(443)_e / I(93)_e\right) + \left(I(501)_e / I(93)_e\right) - 1\right] \alpha_{93} = \left[1 - \left(I(501)_\gamma / I(93)_\gamma\right) - \left(I(443)_\gamma / I(93)_\gamma\right)\right] \qquad 6+$$

$$\left[\left(I(57)_e / I(93)_e\right) - \left(I(443)_e / I(93)_e\right)\right] \alpha_{93} = \left[\left(I(443)_\gamma / I(93)_\gamma\right) - \left(I(57)_\gamma / I(93)_\gamma\right)\right] \qquad 8+$$

where electron intensities include the total of all subshell conversion electron intensities for the transition in question.

Ideally, α_{93} would be the only unknown quantity in the four equations. However, as previously mentioned, the gamma-ray intensity of the 501.0-kev transition was not determined with sufficient accuracy. Because of this, the 6+ level equation contains two unknown quantities, α_{93} and $I(501)_\gamma / I(93)_\gamma$. In addition, the uncertainties of the 443.5-kev transition intensities were quite large. For this reason, this equation was not used in the least-squares adjustment. The remaining equations, nevertheless, constitute three equations in one unknown.

These three equations were therefore used for the spectrometer calibration and absolute conversion coefficient determination. The 6+ level equation was then used to determine the gamma-ray intensity of the 501.0-kev transition.

To determine the deviation from the E^{-2} law, the raw data were corrected for all known correction factors and for a pure E^{-2} crystal reflectivity. These relative intensities, indicated by primes, were then multiplied by a correction function with a parameter, x, indicating the deviation from a pure E^{-2} reflectivity law. As x was expected to be small, the exponential was expanded in a power series with the higher terms being neglected.

$$I(i)_\gamma / I(j)_\gamma = \left[I'(i)_\gamma / I'(j)_\gamma\right] (E(j)/E(j))^x = \left[I'(i)_\gamma / I'(j)_\gamma\right] (1 + x \log E(i)/E(j)) \qquad (11)$$

This was then substituted for the relative gamma-ray intensities in the equations on levels 2+, 4+, and 8+ which then became three equations with two unknown quantities. The equations are of the form

$$a_i \alpha_{93} + b_i x + c_i = 0. \qquad i = 1, 2, 3 \qquad (12a)$$

where a_i, b_i, and c_i are imprecise parameters which are functions of the primitive, uncorrelated data. A least-squares procedure was applied to these equations, taking into account the correlations between the parameters.* The resulting values for the unknowns are $x = -0.026 \pm 0.032$ and $\alpha_{93} = 5.05 \pm 0.29$. The internal errors are given. The ratio of the external and internal error is 1.1, so the data seem consistent.

---

* I wish to acknowledge the kind assistance of Dr. E. R. Cohen who outlined the proper least-squares procedure to use in solving the equations.

D. CONCLUSIONS ON SPECTROMETER CALIBRATION

The values of x obtained from the two calibration methods are in reasonable agreement. That obtained from the Se^{75} experiment alone is 0.000 ± 0.032 which overlaps the value obtained from the Hf^{180} experiment above. A more precise value of x and α_{93} was found by combining the results of the two experiments. This amounts to adding to Eqs. (12a) a fourth equation

$$x - c_4 = 0 \qquad (12b)$$

where c_4 is the value for x obtained from the Se^{75} experiment. The least-squares adjusted values of the variables from this new set of equations are $x = 0.013 \pm 0.022$ and $\alpha_{93} = 5.14 \pm 0.24$. In this case, the ratio of external and internal error is 0.8. The values of the variables were then substituted into the 6+ level equation to obtain the gamma-ray intensity of the 501.0-kev transition as given in Table III. The absolute value of α_{93} was used to establish the scale for the Hf^{180} conversion coefficients in Table IV. These coefficients will be discussed further in Part IV.

The energy dependence of the peak reflection coefficient of the (310) planes in the 2-mm thick quartz slab bent to a 2-meter radius of curvature used in the curved-crystal spectrometer over the range 60 kev $\leq E \leq$ 400 kev is $E^{-1.987 \pm 0.022}$. It is interesting to note that the uncertainty in the value of the exponent includes the number 2.000 within a standard deviation. Thus, the E^{-2} law predicted by Lind et al. does not disagree with the present result. Fig. 12 gives a graph of the correction to a pure E^{-2} law. It also gives the error introduced when correcting relative gamma-ray intensities for the curved-crystal reflectivity. From the figure, it can be seen that the relative uncertainty due to the reflectivity correction when comparing intensities

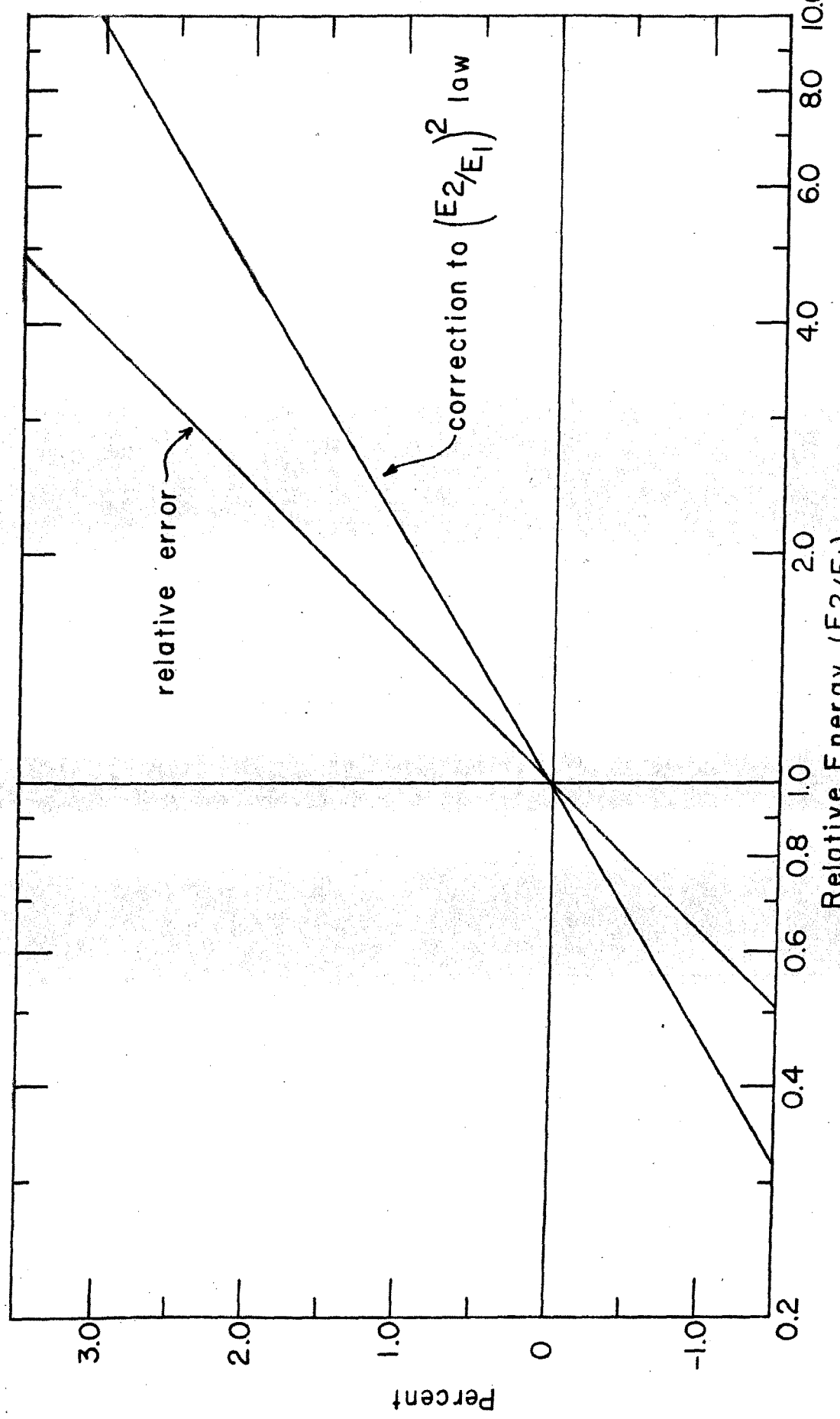

Figure 12. Results of the curved-crystal spectrometer calibration showing the percentage deviation of the $(E_2/E_1)^{1.987} \pm 0.022$ reflection coefficient corrections of the curved quartz crystal (310 planes, 2 mm thick) from a pure $(E_2/E_1)^2$ correction for two gamma rays with energies E_1 and E_2. Also given is the uncertainty in relative intensity measurements arising from uncertainty in the reflectivity law.

of gamma rays whose energies differ by a factor of four has now been reduced to 3%.

PART IV

CONVERSION COEFFICIENTS IN SOME DEFORMED NUCLEI

Using the curved-crystal spectrometer, now calibrated for gamma-ray intensity measurements, and the two beta-ray spectrometers, a study was made of conversion coefficients of transitions in some nuclei within the deformed region. The deformation parameter, δ, measures the eccentricity of the potential in which the nucleons are assumed to move. Measurements of this quantity have been obtained from the intrinsic nuclear quadrupole moment, Q_o, which depends upon the deformation in the following manner, as given by Mottelson and Nilsson (32):

$$Q_o = (4/5)\,\delta\, Z\, R_o^2\, (1 + 1/2\,\delta + \cdots). \qquad (13)$$

where R_o is the mean charge radius of the nucleus.

In deformed nuclei, rotational excited states are found. For even-even nuclei, a zero order formula for the energy levels of an axially symmetric rotating nucleus is

$$E_I = (h^2/2J)\left[I(I+1) - K^2\right] + (h^2/2J_3)K^2 \qquad (14)$$

where J and J_3 are the moments of inertia parallel and perpendicular to the symmetry axis, I represents the total angular momentum and K is the projection of I on the symmetry axis (33). For odd-A nuclei, the formula is similar. The ground-state and also other "intrinsic states" originating from single-particle excitations may give rise to such a rotational band. The spins of the excited states are dependent upon the K quantum number for the group of rotational levels, which is equal to the spin, I, of the intrinsic state upon which the rotations are based. For states based upon K = 0, I takes on the values K, K + 2, K + 4 ... . When $K \neq 0$, the spins of the rotational states are given by I = K, K + 1, K + 2 ... .

Nilsson and Rasmussen have pointed out (11) that anomalous conversion coefficients are to be expected in transitions which are highly

retarded over the single-particle estimates. Since many retarded transitions are found in deformed nuclei, efforts were made to measure conversion coefficients in some of them.

Regions in which deformed nuclei appear are $A = 25$, $150 \leq A \leq 190$ and $A \geq 230$. The nuclei chosen for this study were Hf^{180}, Re^{187}, W^{182}, and W^{183}. Hf^{180} represents a highly deformed even-even nucleus ($\delta = 0.25$) and exhibits four rotational states when decaying from Hf^{180m}. W^{182} is also even-even and has a deformation parameter of 0.23. W^{183} is an example of an odd-A nucleus having a deformation ($\delta = 0.21$). These two tungsten isotopes have many rotational states based on a number of intrinsic states. Re^{187} is another odd-A nucleus and is interesting as it appears at the edge of the strongly deformed region with $\delta = 0.19$. The applicability of nuclear models, based upon deformed potentials, to this nucleus has been under question (34).

The discussion will proceed with a description of the experiments performed and the results obtained with each of these nuclei.

A. Hf^{180} Conversion Coefficients

Introduction and Experimental Method

Fig. 9 shows the decay scheme of Hf^{180m}. The first four excited states are of an almost pure rotational character based upon the ground state with $K = 0$. All of the transitions between these states are E2's. The next excited state is the isomeric 9- state with a half-life of 5.5 hours. The transitions de-populating this state are an E1 to the 8+ level and an E3 to the 6+ level. These transitions are of particular interest. The E1 is retarded by a factor of 10^{15} over the single-particle estimate and is the most highly retarded E1 known. This retardation has already been attributed to K-forbiddenness (35) with

$\Delta K = 9$. Scharff-Goldhaber, et al. have reported (10) (35) on the anomalous nature of the conversion coefficients of this transition. Gvozdev and Rusinov have also made conversion coefficient determinations in this nucleus (36). They have reported K-conversion coefficients for all of the transitions which are converted in the K shell, and have reported values for the L-conversion coefficients of the 443.8-, 93.33-, 57.54-kev transitions.

The methods used in determining the coefficients and their absolute normalization are described in detail on pp. 35-45. The absolute conversion coefficients thus obtained are given in Table IV with the values of Gvozdev and Rusinov and the recent theoretical values of Rose (6) also being given.

Results

The anomalous value of the 57.54-kev L-conversion coefficient is confirmed. Scharff-Goldhaber, et al. report the ratios $L_I/L_{II}/L_{III}$ = 5:0.5:1 which gives $(L_I + L_{II})/L_{III} = 5.5$. The present work gives the same value for the last ratio, 5.5 ± 0.8. According to Rose's theoretical coefficients, the ratios should be $L_I/L_{II}/L_{III} = 1.82/0.81/1$ and $(L_I + L_{II})/L_{III} = 2.63$. Gvozdev and Rusinov report a value for $(L_I + L_{II})/L_{III}$ of approximately 3. Fig. 10 shows the 57.54-kev L-conversion lines. From the figure, it can be seen that L_I gives the main contribution to the composite in agreement with Scharff-Goldhaber. The value obtained for the total L-conversion coefficient is 0.54 ± 0.04, while Scharff-Goldhaber, et al. give 0.4 and Gvozdev and Rusinov give 0.33 ± 0.10. The curved-crystal spectrometer made it possible to resolve the 57.54-kev line from the Hf K x rays, so the gamma-ray intensity was subject to fewer errors. A small amount of M2 admixture might appear to be permissible as the measured $\alpha_{L_{III}}$ is 0.084 ± 0.012

TABLE IV. Data for transitions in Hf^{180m}

Gamma-ray energy (kev)	Gamma-ray intensity (relative units)	Conversion line	Conversion electron intensities (relative units)	Conversion coefficients: Absolute, by present experiment[a]	Conversion coefficients: Experiment by Gvozdev and Rusinov (35)	Conversion coefficients: Theoretical (ϵ)	
						E1	M2
57.54	291 ± 7	$L_I + L_{II}$	0.248 ±0.014	0.458 ±0.036		0.163	69
		L_{III}	0.045 ±0.006	0.084 ±0.012		0.062	22
		L_{total}	0.294 ±0.012	0.543 ±0.036	0.33 ±0.10	0.225	91
		M	0.072 ±0.007	0.134 ±0.015		0.036[c]	43
		N + O	0.012 ±0.002	0.023 ±0.004			
		total	0.378 ±0.013	0.698 ±0.045			
						E2	
93.33	100 ± 2	K	0.205 ±0.012	1.10 ±0.09	1.3 ±0.4	1.03	
		$L_I + L_{II}$	0.343 ±0.017	1.85 ±0.13		1.46	
		L_{III}	0.239 ±0.013	1.29 ±0.09		1.32	
		L_{total}	0.582 ±0.017	3.13 ±0.19		2.80	
		M + N +···	0.169 ±0.012	0.909 ±0.08			
		total	0.956 ±0.023	5.14 ±0.24[a]			
						E2	
215.25	500 ± 14	K	0.114 ±0.005	0.123 ±0.009	0.15 ±0.05	0.138	
		L_{total}	0.072 ±0.006	0.077 ±0.007		0.067	
		total	0.221 ±0.010	0.237 ±0.01			
						E2	
332.5	567 ± 24	K	0.0400 ±0.0016	0.038 ±0.003	0.055 ±0.014	0.042	
		L_{total}	0.0154 ±0.0012	0.0146±0.0015		0.0130	
		total	0.0634 ±0.0025	0.0603±0.004			
						E2	
443.8	491 ± 26	K	0.0173 ±0.0010	0.0189±0.0017	0.026 ±0.007	0.020	
		L_{total}	0.0040 ±0.0005	0.0044±0.0007	0.0063±0.0016	0.0049	
		M + N +···	0.00141±0.00028	0.0015±0.0003			
		total	0.0227 ±0.0012	0.0249±0.0022			
						E3	M4
501.3	102 ± 31[b]	K	0.0070 ±0.0009	0.0370±0.012	0.035 ±0.014	0.040	0.77
		total	0.0104 ±0.0011	0.0549±0.018			

a. The normalization of these conversion coefficients was fixed by a_{93} whose absolute value was determined as described on pp. 35-48.

b. This value was not measured directly but was deduced from the feeding and bleeding of levels as discussed on page 46.

c. Not corrected for screening.

TABLE V. Subshell intensity ratios of conversion electrons for transitions in Hf^{180m}

Gamma-ray energy (kev)	Subshell ratios Identification	Measured value	Theoretical value (6)	
			E1	M2
57.54	$(L_I + L_{II})/L_{III}$	5.5 ± 0.8	2.63	3.13
	L/M	4.1 ± 0.4	2.62	2.12
	L/(N+O ...)	24 ± 4	-	
			E2	
93.33	K/L	0.352± 0.025	0.368	
	$(L_I + L_{II})/L_{III}$	1.44 ± 0.10	1.11	
	L/(M+N ...)	3.44 ± 0.26	-	
			E2	
215.25	K/L	1.59 ± 0.14	2.08	
			E2	
332.5	K/L	2.60 ± 0.23	3.20	
			E3	
443.8	K/L	4.3 ± 0.6	4.1	

whereas the theoretical value is 0.062. The amount of M2 admixture needed to bring agreement with $\alpha_{L_{III}}$ is (0.10 ± 0.06)%. However, this would only bring the theoretical value for $\alpha_{L_I} + \alpha_{L_{II}}$ up to 0.24 ± 0.04. Since the measured value for this last quantity is 0.44 ± 0.03, it is clear that the anomalous L-conversion cannot be entirely reconciled by including an M2 admixture. Whether $\alpha_{L_{III}}$ itself is anomalously high or an M2 admixture does exist are questions that cannot be decided at present. The 57.54-kev M coefficient is approximately 60% high. The screening effect, which was neglected in Rose's calculation of the M coefficients, would lower the theoretical value (37). Since the present experimental value is high, a true anomaly seems to exist.

The 501.0-kev E3 transition does not show an anomalous nature within the rather large experimental error.

The E2 transitions show some interesting features. The K-conversion coefficients show a slight trend toward lower values and contradict the trend toward higher values reported by Gvozdev and Rusinov. The total L coefficients show an energy variation with respect to the theoretical values. The experimental coefficients are slightly high at low energies becoming lower as the energy increases. This effect shows up clearly in the K/L ratios given in Table V with the exception of the ratio for the 93.33-kev transition where α_K is somewhat high.

B. Re^{187} Conversion Coefficients

Re^{187} has the smallest deformation ($\delta = 0.19$) in the region of strongly-deformed nuclei, $150 \leq A \leq 190$. One of the aims of this investigation was to obtain good absolute conversion coefficients in this region so, in addition to obtaining energies and relative conversion coefficients of many transitions, considerable effort was made to find an absolute normalization of them.

Many weak transitions occur having an energy above 500 kev where the reflectivity of the curved crystal makes it difficult to obtain sufficient intensity for either good determinations of gamma-ray energies or of gamma-ray intensities. For this reason, an extended gamma source was used with the spectrometer in addition to the usual line sources, as mentioned in Part II. The source absorption correction for the extended source was made using intensities of strong lines measured in both sources, thus finding a curve which would normalize the extended source intensities to the line source intensities. The lines used for the normalization were the 72.00-, 134.25-, 479.4-, 551.7-, 618.2-, 686.1-, and 773-kev gamma rays.

Table VI gives the gamma-ray intensities measured with the curved-crystal spectrometer.

Absolute Normalization of the Conversion Coefficients

First, the measured gamma-ray and conversion-electron intensities were preliminarily normalized so as to yield the theoretical E1 value for the 686-kev transition. The conversion coefficients on this scale were then reduced to an absolute scale by multiplication by a factor y which was determined by three different methods,

1. direct determination of $\alpha_{K_{134.25}}$ by a coincidence experiment,
2. feeding and bleeding of the 134- and 206-kev levels, and
3. comparison of the total number of K holes with the observed K x-ray intensity.

Gallagher et al. (34) measured the K- x rays and 134.25-kev gamma rays in coincidence with the 551.7-kev gamma rays. The ratio of K holes to 134.25-kev gamma rays obtained after correcting the coincidence ratio for the Auger effect, is directly the K-shell conversion

coefficient of the 134.25-kev transition. Their measured value was $\alpha_K = 1.6 \pm 0.3$. Comparison of this with the relative value gave $y = 0.94 \pm 0.21$.

Before methods two and three could be applied, it was necessary to determine the K-conversion coefficient of the strong 72.00-kev transition which was not directly measured, because the K-conversion line was not observed. The procedure by which this was evaluated is discussed in connection with the second method of determining the absolute normalization factor.

Beta branching to the 134.25-kev and 206.25-kev levels was not observed, to within 10% of the intensity of the beta group to the ground state. Because of this, equations relating the decay fractions populating to those de-populating each level could be written. Equations were thus obtained with the unknown quantities being α_{K72} and y. The solutions are $y = 0.96 \substack{+0.17 \\ -0.11}$ and $\alpha_{K72} = 1.01 \substack{+0.14 \\ -0.20}$.

It must be realized that α_{K72} thus obtained is not independent of the final value of the normalization factor. The above value of α_{K72} was obtained from a value of y as determined from the modes of populating and de-populating the levels and not on the final mean value of y as determined from the values obtained by all three methods. This value of α_{K72} in turn affects y in the third method. In essence a least-squares adjustment should be made. The difference, however, between such least-squares adjusted values and those quoted is not expected to be significant as illustrated by the good agreement between the values of y determined by the three methods.

The third method was to determine the number of K holes in Re^{187} from the number of K x rays observed. The number of K holes is equal to the sum of the product of the K-conversion coefficient and the photon

intensity for each transition. (The presence of K x rays from tungsten resulting from the fluorescence excitation of the source material by the beta rays as they pass through the sample does not interfere with the result because the W K x rays and the Re K x rays were clearly resolved. Furthermore, from the very small ratio of W to Re atoms, and from the intensity of the W K x rays, it was estimated that the contribution to the Re K x ray intensity from fluorescence excitation was negligible.)

Difficulty was encountered in consequence of the fact that the natural line width of the K x rays is larger than that of most gamma rays. In most instruments used in gamma-ray spectroscopy, this is of no importance, as the inherent window widths of the measuring instruments are large compared to the natural line width. This is not true for the curved-crystal spectrometer, for whereas the natural width for gamma rays is small compared with the window, that of x rays is not. Consequently, peak heights cannot be used as a measure for x-ray intensities in the same way as for gamma-ray intensities. The direct integration of the Re K α_I x ray and the 72.00-kev gamma ray, correcting for the long tails of the x ray, yielded a correction factor to the K α_I peak height intensity of 1.62 ± 0.03. A second method depended upon a knowledge of the shape and half-width of the natural x-ray line and the shape of the instrument window. This yielded a value of 1.6 and served as a check on the previous more precise value. A full discussion of the problems involved and the procedures used is found in App. IV.

The intensity of the K-α_1 x ray thus obtained on the same scale as the gamma ray intensities is 49 ± 2. The K-α_2 and K-β x rays were also measured but not as accurately. The correction for their contribution was estimated by using the ratio of their intensities to the intensity

of the K-α_1 as reported in Wapstra et al. (24). The ratios are $K\beta_1\beta_3/K\alpha_1 = 0.335 \pm 0.01$, $K\beta_2/K\alpha_1 = .84 \pm 0.005$ and $K\alpha_2/K\alpha_1 = 0.543 \pm 0.015$.

Using the fluorescence yield of 0.947 as interpolated from the values of Wapstra et al., the total K x ray intensity as obtained above, and the summation of the product of the K-conversion coefficient times the photon intensity for each transition, the normalization constant is obtained; $y = 0.85 \begin{smallmatrix}+0.09\\-0.11\end{smallmatrix}$.

The mean of the values of y of the three different methods was taken to be 0.89 ± 0.08. The ratio of the external error to the quoted internal error is 0.5 indicating good consistency of the data. This normalization factor was used to obtain the absolute conversion coefficients which are listed in Table VI.

Conversion Coefficients

The high energy transitions, as shown in Table VI, have conversion coefficients which agree, in general, with pure multipolarity assignments. Still, in almost every case, the experimental value is somewhat lower than the theoretical although the latter is usually within the quoted standard deviation. A systematic normalization error would account for this discrepancy but its existence seems improbable.

The 134.25-kev transition appears to be an M1 + E2 mixture. α_K for this transition is 1.5 ± 0.2 whereas the theoretical value is 1.93. The present measurement is in agreement with that of Vergnes (38) who obtained $\alpha_K = 1.5 \pm 0.4$.

The K-conversion coefficient of the 72.00-kev transition is interesting. As previously mentioned, the K-electron intensity was not measured, as the energy of the electrons is only 0.34 kev. The K-conversion coefficient was, however, determined from the feeding and

bleeding of levels, the value obtained being $\alpha_K = 1.01 \, ^{+0.14}_{-0.20}$. The theoretical value for a pure E1 is 0.52. M2 mixing would not be a reasonable way to resolve the anomaly, for the L_I and L_{II} coefficients are lower than the theoretical E1 values (L_{III} was not measured as it was not resolved from the 134.25-kev K-electron line). $\alpha_{L_I} = 0.055 \pm 0.007$ and $\alpha_{L_{II}} = 0.019 \pm 0.004$ while the theory gives $\alpha_{L_I} = 0.068$ and $\alpha_{L_{II}} = 0.030$. If the present assumption, that beta feeding of the 206.2-kev and 134.25-kev levels is less than 10% of that to the ground state, is true, then suspicion might be cast upon the theoretical value.

The question is logically raised as to the validity of the theory for a transition whose energy differs so little from the binding energy of the electrons being considered. Spinrad (39) has tabulated values for threshold conversion coefficients. At an energy corresponding to the K-binding energy of rhenium, his E1 conversion coefficient is 0.67. There is also some question as to the validity of his theory, for the calculations were made under the assumptions of a point nucleus and no screening. Indeed, they depend upon limiting values of the earlier point nucleus calculations of Rose et al. (1). The present results support the conclusion that existing theoretical conversion coefficients may not be extrapolated to the limiting threshold energies.

C. W^{182} and W^{183} Conversion Coefficients

Introduction

In 1954, Murray et al. (13) (40) reported the results of a very complete study of the decay schemes of Ta^{182} and Ta^{183}. These isotopes decay by negative beta emission into tungsten. The proposed level scheme of W^{182} was later interpreted by Alaga et al. (41) in terms of different rotational bands. Later, however, questions were raised with

TABLE VI. Data for transitions in Re^{187}

Gamma-ray energy (kev)	Gamma-ray intensity	Experimental conversion coefficients[a] α_K	α_{L_I}	$\alpha_{L_{II}}$	$\alpha_{L_{III}}$	Multipolarity assignments	Theoretical conversion coefficients[b] α_K	α_{L_I}	$\alpha_{L_{II}}$	$\alpha_{L_{III}}$	Decay fraction[c] (%)
72.00±0.01	49.7 ±1.9	1.01 $^{+0.14}_{-0.20}$	0.055±0.007	0.019±0.004[d]		E1	0.52	0.068	0.030	0.033	27
96.0 ±0.5[ef]	≤0.12	≥4				-[g]					
106.61±0.06	0.17±0.02	2.9 ±0.6				M1(+E2)	3.70(0.74)				0.13
113.74±0.05	0.36±0.03	2.9 ±0.7				M1(+E2)	3.20(0.68)				0.26
134.25±0.02	40.0 ±1.2	1.5 ±0.2	0.30 ±0.04	0.040±0.005	0.010±0.002[h]	M1 + E2	2.05(0.49)	0.265(0.048)	0.0238(0.340)	0.00265(0.283)	33
206.2 ±0.2	0.48±0.05	2.1 ±0.3	0.6 ±0.2			M2	2.50	0.55	0.069	0.064	0.50
239.3 ±0.3	0.34±0.05	0.6 ±0.3				M1(+E2)	0.375(0.103)				0.16
246.3 ±0.3	0.52±0.05	0.3 ±0.1				M1 + E2	0.345(0.095)				0.20
479.4 ±0.4	100	0.014 ±0.002	α_L = 0.0039 ± 0.0005[i]			E2	0.0185	α_L = 0.0048			28.5
511.3 ±0.7	2.6 ±0.2	0.012 ±0.003				E2	0.0158				0.73
529 ±3[e]	≤0.4	≥0.04				-[g]					
551.7 ±0.7	21.2 ±0.7	0.0050±0.0007				E1	0.0051				5.9
618.2 ±0.6	26 ±1	0.027 ±0.004				M1	0.031				7.5
625.1 ±1.6	4.3 ±0.2	0.009 ±0.004				E2	0.0104				1.2
686.1 ±0.4	116 ±5	0.0029±0.002				E1	0.033				32
773 ±1	16.2 ±0.8	0.016 ±0.003				M1	0.0177				4.6
867 ±3	1.53±0.25	0.013 ±0.006				M1	0.0130				0.43

Footnotes for Table VI on page 62.

a. These are absolute coefficients. The normalization is discussed in the text.

b. The theoretical coefficients are those by Rose (6) and are for the multipolarity assignments given in column 7. Coefficients given between parentheses are the theoretical E2 values for gamma rays which are assigned as M1 + E2 mixtures.

c. The decay fraction is proportional to $(1 + \alpha_{total})I_\gamma$ and is normalized assuming 20% primary beta branching to the ground state.

d. $\alpha_{L_I}/\alpha_M/\alpha_{(N+O)} = 1/0.3/0.1$.

e. The energy was deduced from the electron line only.

f. The K-line of a 96.0-kev transition can possibly be assigned as the L-line of a 36.2-kev transition.

g. The limit on the conversion coefficient rules out E1 or E2.

h. $I_{L_I}/I_M/I_N/I_O = 1/0.24/0.07/0.02$.

i. $I_L/I_M/I_{(N+O\ \ldots)} = 67/28/11$.

regard to the conversion coefficients and the multipolarity assignments of the transitions. Murray et al. had normalized the conversion coefficients to the theoretical value for a pure M1 for the 246.05-kev transition in W^{183} using the point-nucleus theoretical coefficients of Rose et al. (1). This assignment was made on the basis of the L subshell ratios of Gellman et al. (42). With this normalization, a number of transitions whose coefficients were too large to be pure E2's were assigned as M1 + E2 mixtures. Some, such as the 229.27-kev and 264.09-kev transitions in W^{182}, were assigned as E2 even though their conversion coefficients indicated a considerable M1 admixture.

After an analysis of Murray's values, Wapstra and Nijgh (2) concluded that the normalization was incorrect. Changing the normalization so that the E2 transitions agreed in the average with the theoretical E2 coefficients, they found that the M1 transitions were then generally lower than the theoretically predicted values of Rose. This, they concluded, was due to a finite nuclear size effect predicted by Sliv and Listengarten (4) which would cause a greater deviation in the M1 coefficients than in the E2 coefficients. This conclusion was shown to be correct with the appearance of the coefficients of Sliv and Band (5).

However, the situation was still not completely resolved. Some coefficients, such as α_K for the 152-kev transition, were still anomalous as pointed out by Nilsson and Rasmussen (11). In addition, Froman and Ryde (43) made a coincidence study of the W^{182} decay. Using scintillation methods, they reported disagreement between their gamma-ray intensities and those of Murray et al. Indeed, they reported that agreement could be obtained if the intensities of Murray et al. were multiplied by a function which varied in a fairly smooth manner with the gamma-ray energy.

Because of the interest that has arisen in connection with the conversion coefficients of the W^{182} and W^{183} isotopes, and since there was reason to doubt the gamma-ray intensities of Murray et al., it was felt that a remeasurement of these intensities was in order. With the curved-crystal spectrometer calibrated for intensity measurements, this project was undertaken. As there was little reason to be suspicious of Murray's beta-spectrometer measurements, conversion electron intensities were not remeasured.

The 5-day W^{183} gamma rays were measured shortly after receiving the activated source. After determining the intensities in this isotope, the W^{183} activity was allowed to decay considerably before measuring the 112-day W^{182} gamma-ray intensities, thus reducing the background considerably. As energy measurements were previously made by Murray et al., these were repeated for a few gamma rays only as a check.

Results

In the case of the W^{182} gamma-ray intensities, the conclusions of Froman and Ryde are confirmed. The new intensity measurements differ from those of Murray et al. by a factor which varies in a fairly smooth manner with the energy. Table VII gives the gamma-ray intensities. Fig. 13 shows the variation between the present gamma-ray intensities and those of Murray et al. and of Froman and Ryde. From the curve, it can be seen that the present values agree in general with those of Froman and Ryde. With the single exception of the 67.74-kev transition, intensity agreement is within 20%, and most of the intensities agree within 10%. On the other hand, some of the present intensity figures differ with those of Murray et al. by as much as a factor of two. This discrepancy cannot be attributed to reflection coefficient corrections, for the correction Murray used ($E^{-2.000}$) has now been shown to be within

the experimental error. Source absorption is a possible cause of the error as the source absorption of the low-energy gamma rays was as much as 90%.

The same energy dependent discrepancy factor that was found in the W^{182} intensities was naturally expected in the gamma-ray intensities from W^{183} (Table VIII) since only one source was used for measurements in the two isotopes, both in the present experiment and that of Murray et al. Nevertheless, this very marked energy dependence was not observed. Fig. 14 shows the ratio of the intensities of Murray et al. and the present values. With the exception of the two very high points at 365.60 kev and 406.58 kev, there seems to be little consistent variation with energy. If the variation does exist, the slope of the curve is certainly less than in the case of W^{182}.

Conversion coefficients were determined from the present gamma-ray intensities and the conversion electron intensities of Murray et al. as obtained from published data (13). However, the reported electron intensities were re-corrected for window absorption as there was reason to believe that the correction curve determined by Murray (40) was incorrect. He had used the continuous beta spectrum from Cs^{137} to determine the correction. Their results differed markedly with those published later by Slatis (19). The present correction was based on curves given by Slatis for 1.0 mg/cm^2 mica windows which were interpolated to obtain the correction for a 1.1 mg/cm^2 window, which was the effective thickness of the window used by Murray et al.

The conversion coefficients are given in Tables VII and VIII. Error assignments were not made as conversion electron uncertainties were not included in Murray's published data and it was not possible to retrace them. The theoretical values of Rose (6) are also given for

TABLE VII. Data for transitions in W^{182}

Gamma-ray energy (kev)	Gamma-ray relative intensity (kev)	Measured Internal Conversion Coefficients [a,b] α_K	α_{L_I}	$\alpha_{L_{II}}$	$\alpha_{L_{III}}$	Multipole order [c]	Theoretical Internal Conversion Coefficients [d] α_K	α_{L_I}	$\alpha_{L_{II}}$	$\alpha_{L_{III}}$
33.36	<0.2[e]									
42.71	0.71± .04									
65.71	8.7 ±0.4		1.1	0.2	0.09	M1		1.87(M1)	.160(M1)	.022(M1)
67.74	139 ± 7		0.06	0.02	0.08	E1		0.079	0.033	0.041
84.67	7.8 ±0.4		0.5	0.2	0.14	M1		0.88(M1)	0.075(M1)	0.0100(M1)
100.09	40	0.47	0.05	0.6	0.5	E2	0.70	0.094	1.13	1.03
113.66	5.3 ±0.3	1.0	0.2	0.04		M1	2.7	0.37	0.032	
116.40	1.25±0.07									
152.41	20.2 ±0.8	0.05				E1	0.11			
156.37	8.2 ±0.4					E1				
179.36	9.2 ±0.4	0.27	0.10		0.03	E2 + M1				
198.31	4.3 ±0.3	0.15		0.07	0.04	E2	0.17	0.019	0.053	0.053
222.05	22.6 ±0.9	0.03	0.005			E1	0.041			
229.27	11.1 ±0.5	(.102)[b]		0.03	0.02	E2	0.102	0.014	0.028	0.028
264.09	10.9 ±0.5	0.08		0.03	0.01	E2	0.082	0.010	0.015	0.015

a. These coefficients were calculated using the electron data of Murray et al. (13) for all of their reported electron transitions.

b. The relative conversion coefficients were normalized to the theoretical E2 value for the K-conversion coefficient of the 229.27-kev transition.

c. The assignments are those given by Alaga et al. (41).

d. These are Rose's theoretical values (6) for the multipole order given in column 7.

e. This transition was reported by Murray et al. (13) but was not observed in the present experiment.

TABLE VIII. Data for transitions in W^{183}

Gamma-ray energy (kev)	Gamma-ray relative intensity	Measured internal conversion coefficients[a,b] α_K	α_{L_I}	$\alpha_{L_{II}}$	$\alpha_{L_{III}}$	Multipole order	Theoretical internal conversion coefficients[d] α_K	α_{L_I}	$\alpha_{L_{II}}$	$\alpha_{L_{III}}$
40.97	0.73±0.04		21		1.9	M1		6.55	0.62	0.090
46.48	17.2 ±0.9		8.6	0.13	0.6	M1		4.8	0.435	0.061
52.59	17.6 ±1.0		5.2	1.3	0.8	M1		3.47	0.306	0.0426
82.92	1.78±0.13		1.0			(M1)		0.94		
84.70	12.4 ±0.7		0.7			M1		0.88		
99.07	23.3 ±1.4	0.9		1.5	1.4	E2	0.81	0.097	1.20	1.10
101.94	1.3 ±0.1	3.6				M1	4.19			
102.49	0.71±0.08	18	3.5			M2	28.6	7.3	0.8	1.7
103.14	1.02±0.11					(E2)				
107.93	36.9 ±2.2	3.7	0.6			M1	3.60	0.45		
109.73	2.07±0.13					(M1)	3.48			
120.38	0.23±0.04	3.0				M1	2.75			
142.25	1.31±0.11		0.38			M1	1.75	0.195		
144.12	10.2 ±0.7	1.52	0.24			M1	1.66	0.190		
160.53	10.8 ±0.5	0.4				E2	0.316			
161.36	31.6 ±1.3	1.15				M1	1.20			
162.3	17.9 ±0.6	1.0				M1	1.18			
192.64	1.18±0.07	0.47				M1	0.69			
203.27	1.42±0.09	0.39				M1	0.59			
205.06	3.03±0.14	0.7	0.13			M1	0.58	0.070		
208.81	2.5[e]	0.7				M1	0.55			
209.87	15.9 ±0.8	0.21		0.061	0.3	E2	0.148	0.0170	0.0410	0.0290
244.26	32.9 ±1.6	0.14				E2	0.098			
246.05	100	(0.345)	0.061			M1	0.345	0.0422		
291.71	28.9 ±1.4	0.04		0.014		E2	0.061	0.0082	0.010	0.0060
313.03	26.2 ±1.3	0.22	0.033			M1	0.180	0.0222		
354.04	41 ±3	0.12	0.020			M1	0.131	0.0157	0.001	
365.60	1.53±0.08					(M1)				
406.58	2.00±0.11					E2				

a. These coefficients were calculated using the electron data of Murray et al. (13) for all of their reported transitions.

b. The relative conversion coefficients were normalized to the theoretical M1 value for the K-conversion coefficient of the 246.05-kev transition.

c. The multipolarity assignments are those given by Murray et al. (13).

d. These coefficients are Rose's theoretical values (6) for the multipole order given in column 7.

e. This intensity was obtained from the present value for the 209.87-kev transition and Murray's intensity ratio for the two transitions.

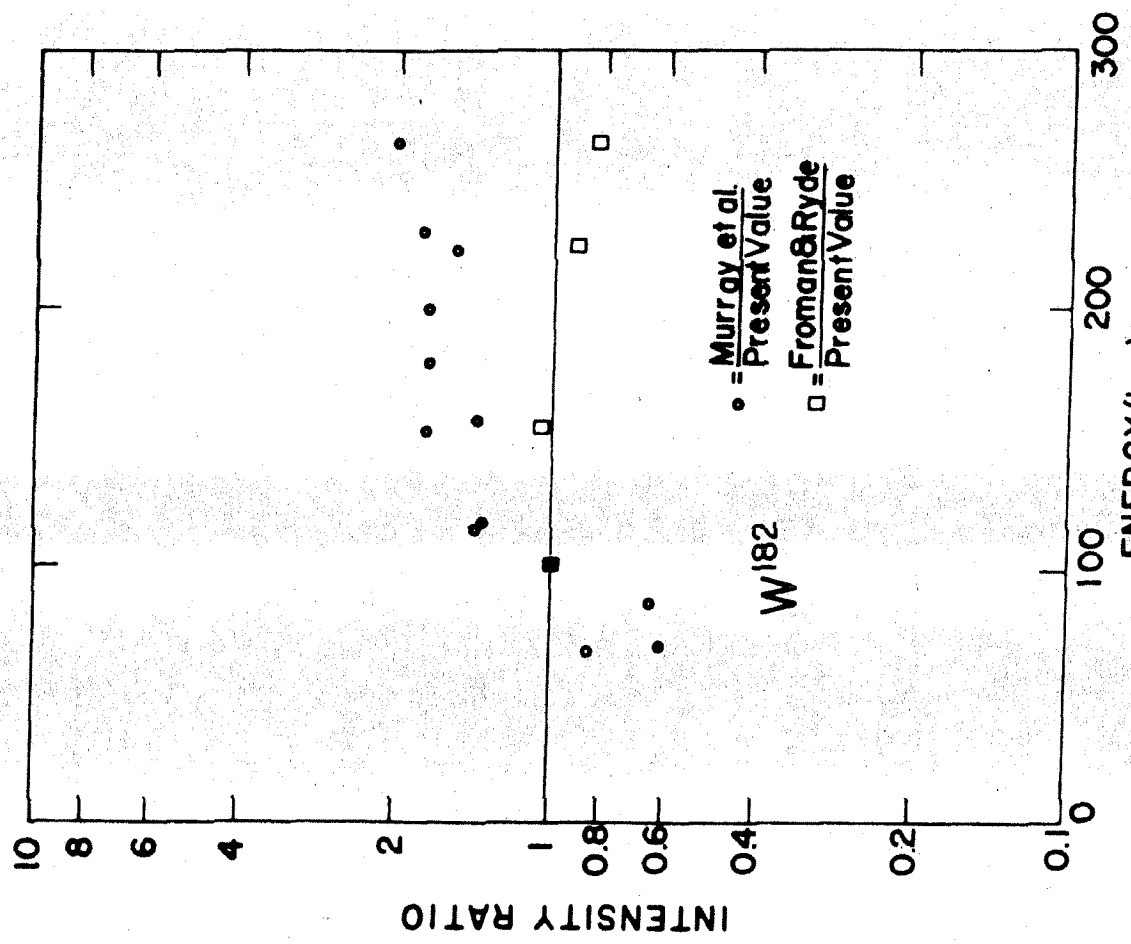

Figure 13. Present gamma-ray intensities in W^{182} relative to those determined by other authors.

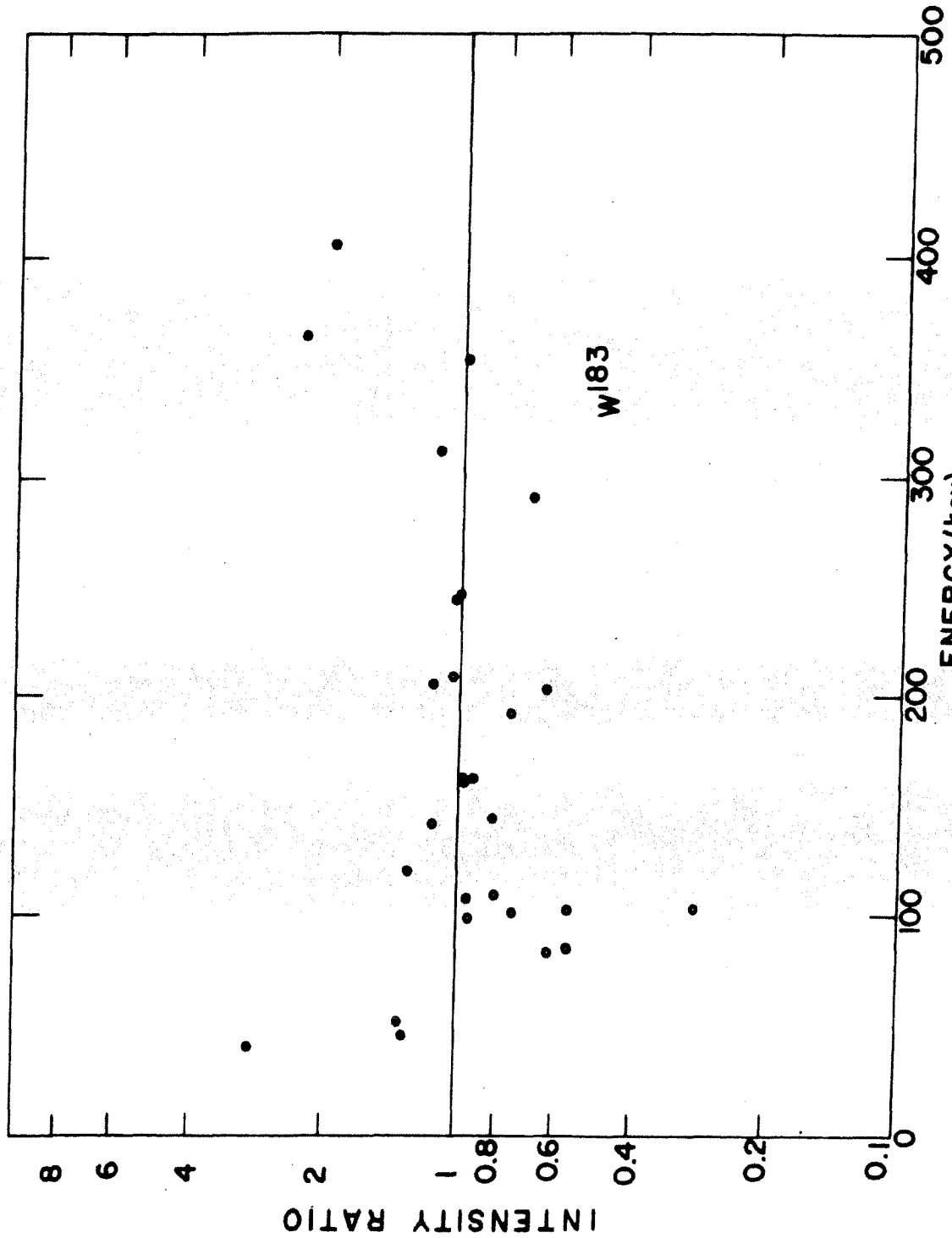

Figure 14. Present gamma-ray intensities in W^{183} relative to those determined by Murray et al. (10). The ratio is Murray's values divided by the present determinations.

comparison. The theoretical coefficients correspond to the transition assignments of Alaga et al. (41) for W^{182} and Murray et al. for W^{183}. The W^{182} experimental conversion coefficients were normalized to the theoretical E2 value for the 229.27-kev transition; the W^{183} values were normalized to the theoretical M1 value for the 246.05-kev transition. Strong high-energy transitions were chosen for normalization to avoid beta-window absorption errors.

Discussion

W^{182}: The agreement with theoretical values is generally reasonable. A trend toward low conversion coefficients (with respect to the theoretical values) might exist at low energies. This is certainly the case if the 65.71-kev and 84.67-kev transitions are pure M1 as suggested by Alaga et al. However, the L-subshell values indicate that E2 admixture might be present. Indeed, it is difficult to reconcile the very large values of $\alpha_{L_{III}}$ in both cases with a pure M1 assignment. An E2 admixture would lower the value of L_I and raise the values of L_{II} and L_{III} in agreement with the observed subshell coefficients.

According to the present normalization, the conversion coefficient for the 152.41-kev transition is less than half the theoretical value for a pure E1. This is in further confirmation of anomalous E1 conversion for this transition as discussed by Nilsson and Rasmussen(11).

W^{183}: The conversion coefficients of transitions having moderate or high energies are generally in agreement with the assignments although there is considerable scatter about the theoretical values. It is felt that this should be interpreted as reflecting errors in the measurements. In addition to the scatter, as the energy increases, the conversion coefficients tend toward higher than theoretical values.

This would be explained by the trend of the gamma-ray intensity ratios as shown in Fig. 14 if the gamma-ray intensities of Murray et al. were assumed to be correct. But this is in contradiction with the results found in W^{182} where the disagreement with Murray's results is more striking and the present values are in agreement with those of Froman and Ryde. There is, however, further evidence that the present gamma-ray intensities in W^{183} might be wrong. If Murray's gamma-ray intensities were correct, the L-shell conversion coefficients of the low energy transitions would not be so anomalously high.

The solution of this difficulty with its contradictory implications has not been found. Further studies of the electron intensities are certainly in order. In addition, the low energy gamma-ray intensities might be checked with very thin sources where source absorption would be negligible.

D. Discussion and Summary

As a result of this study, conversion coefficients have been obtained which, through transition multipolarity assignments, have aided the study of a number of decay schemes. The Se^{75} radioactive isotope, although not in the region of deformed nuclei, was studied in connection with the spectrometer calibration and yielded conversion coefficients which were helpful in establishing the character of the decay scheme. This decay is discussed in Appendix II.

The Hf^{180} conversion coefficient study has yielded anomalous conversion coefficients for the 57.54-kev E1 transition. In addition, a study of the transition energies has resulted in determinations of rotational levels which deviate from the two parameter formula. Indeed, precision energy measurements indicate that the theory does not correctly

predict the energy of any of the higher levels in Hf^{180}. Appendix I discusses this in detail.

The Re^{187} nucleus was studied in detail. From conversion coefficient measurements, multipolarity assignments for most of the transitions were made. Using these assignments and precise gamma-ray energy measurements, the decay scheme was more fully analyzed as discussed in Appendix III.

Studies of W^{182} gamma-ray intensities have resulted in more precise values of the conversion coefficients and indicate a deviation from the results of Murray et al. (13) (40). The multipolarity assignments of Alaga et al. (41) have generally been confirmed.

W^{183} gamma-ray intensity measurements indicate the need for further study of this isotope. Conversion coefficients are only in general agreement with suggested multipolarity assignments and show an energy dependent deviation which has not been fully explained. Further conversion electron measurements should probably be made.

Anomalous Conversion Coefficients

Anomalous conversion of some transitions in deformed nuclei has been confirmed and coefficients of other transitions not previously reported as anomalous have been found to deviate from the present theoretical values. A discussion of transitions in which these anomalies appear follows. The theoretical conversion coefficients are from the recent tables by Rose (6).

Hf^{180m}, 57.54 kev, E1

The $(L_I + L_{II})$ conversion coefficient is high by more than a factor of two which is primarily due to a large value for α_{L_I}. Its value is 0.46 ± 0.04 whereas the theoretical value is 0.16. $\alpha_{L_{III}}$ has a value of

0.084 ± 0.012 which is 30% higher than the theoretical value of 0.062. The M-conversion coefficient is high, almost by a factor of two. α_M = 0.151 ± 0.012 where the theoretical value is 0.086. The fact that the theoretical M coefficients are unscreened does not seem to explain the anomaly, as correction for this effect would increase the discrepancy. M2 admixture cannot account for the deviation of these conversion coefficients from the theoretical E1 values. The conversion anomaly along with the high retardation of this transition ($\sim 10^{15}$) has already been explained as resulting from K forbiddenness.

Hf^{180m}, E2 transitions

The transitions are not forbidden and there is no reason to expect anomalies. Nevertheless, the present measurements indicate deviations from the theory. With the exception of the 93.33-kev transition, the K-conversion coefficients are all about 10% low. With respect to the theoretical values, the L coefficients seem to follow a fairly smooth curve decreasing as a function of energy with the crossing point around 400 kev. With the exception of the 93.33-kev transition, this variation is also evident in the K/L ratios.

Re^{187}, 72.00 kev, E1

The K-conversion coefficient for this transition was determined to be $1.01^{+0.14}_{-0.20}$. Rose's theoretical value for a pure E1 is 0.52; Spinrad's is 0.67. The assumption of an M2 mixture does not bring agreement with the theoretical coefficients in this transition, for the L_I and L_{II} coefficients are lower than the theoretical E1 values. The energy of the K-conversion electrons after leaving the atom is only 0.34 kev. Perhaps the present theories are not valid for conversion in transitions whose energies are very near the binding energy of the electron.

W^{182}, 152.41 kev, E1

Murray et al. reported a K-conversion coefficient for this transition of 0.07 against a theoretical value of 0.11. The anomaly is confirmed with the present measurement of 0.05. Gallagher also attributes anomalous conversion to this transition having measured a K/L_I ratio which is about 1/3 the theoretical value as reported by Nilsson and Rasmussen (11).

APPENDICES

APPENDIX I

Hf^{180} TRANSITION ENERGIES

Introduction

The decay of Hf^{180m} is unique in many respects. It contains the most highly retarded E1 known, which is an isomeric transition of 6.8 hours partial half-life. This E1 also exhibits anomalous internal conversion. In addition, the Hf^{180m} decay scheme is one of the outstanding examples of rotational energy levels. The nucleus is even-even and the ground state has spin 0+; therefore the rotational levels, based on the ground state, have K=0, and the spins and parities of the levels proceed 2+, 4+, 6+, and 8+. The next level with spin and parity of 9- is considered to be the beginning of another rotational band with K=9 which makes the E1 transition from the 9- level to the 8+ level highly K-forbidden.

Hf^{180} Energy Levels

For nuclei with a rotational band based upon K=0 the two parameter formula for the energy levels is

$$E_I = (\hbar^2/2J)\, I(I+1) - BI^2\ (I+1)^2 \qquad (15)$$

where J is the moment of inertia parallel to the symmetry axis, I is the total angular momentum and $BI^2(I+1)^2$ is a correction term which allows for coupling of a vibrational nature to the rotational level and for other second order effects (33). The introduction of this second term to the simple rotation formula brought very good agreement to the energy levels of even-even nuclei at the ends of the regions of high nuclear

deformation where the levels previously deviated from the simple, one parameter rotational formula. Thus, by variation of the two parameters, $\hbar^2/2J$ and B, good agreement between theory and experiment could be established in the regions $150 \leq A \leq 193$ and $A \geq 224$. Up to this time, the Hf^{180} levels, when corrected for rotation-vibration interaction, have given agreement to within experimental errors (44). However, it now appears that a deviation does exist.

The gamma-ray transition energies have been measured with the curved-crystal spectrometer. Figure 15 gives these measurements with the level energies determined from the photon energies. A fit was made to the first three levels using the above formula. The values of the moment-of-inertia parameter and of the vibration-interaction parameter were determined to be $h^2/2J = (15.609 \pm 0.006)$ kev and $B = (0.0090 \pm 0.0005)$ kev.

The energies of the 6+ and 8+ levels, predicted from these values of the parameters, are also shown in the figure. As can be seen, the predicted values are lower than the experimental energies; in addition, there is no overlap of the errors. Although the deviation is only 0.32% on the 6+ level and 0.77% on the 8+ level, it nevertheless appears to be real and significant. Figure 16 shows the relationship between the values and the errors on the predicted and the experimental energies. One should remember that the energy uncertainty for lines measured with the curved-crystal spectrometer is not a standard deviation, but corresponds to at least a 90% confidence limit. Thus the probability of the deviation of the measured energy of the 6+ level being statistical is of the order of 1/100 while that for the 8+ level is smaller yet. What might also be significant is that the deviation seems to be increasing with increasing energy. Whereas the deviation is about two error limits

on the 6+ level, the gap has increased to about three on the 8+ level.

A third order term $C\left[I(I+1)\right]^3$ was introduced into the formula and a fit was made to the 0+, 2+, 4+, and 6+ levels. As might be expected, the predicted 8+ level energy was raised and came into agreement with the experimental value, the predicted energy being 1093 ± 24 kev against an experimental value of 1085.6 ± 0.7. However, the uncertainty in the parameter C was of the order of 100%, which is reflected in the large uncertainty in the predicted level, so it might be said that agreement was reached not so much by bringing the values together as by increasing the error limits.

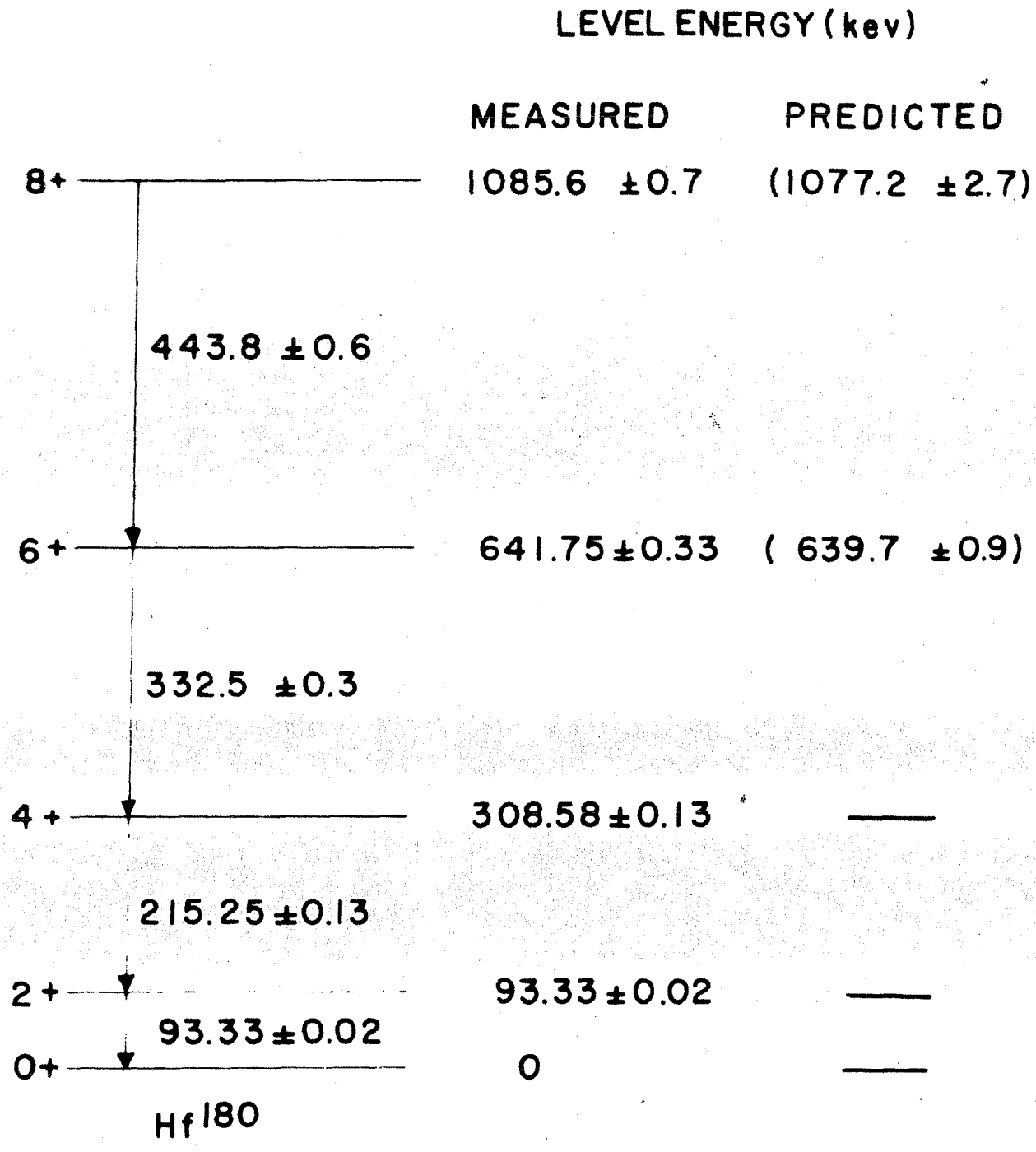

Figure 15. The rotational spectrum of Hf^{180} compared with theoretically predicted values based upon the two parameter formula fit to the 0+, 2+, and 4+ levels.

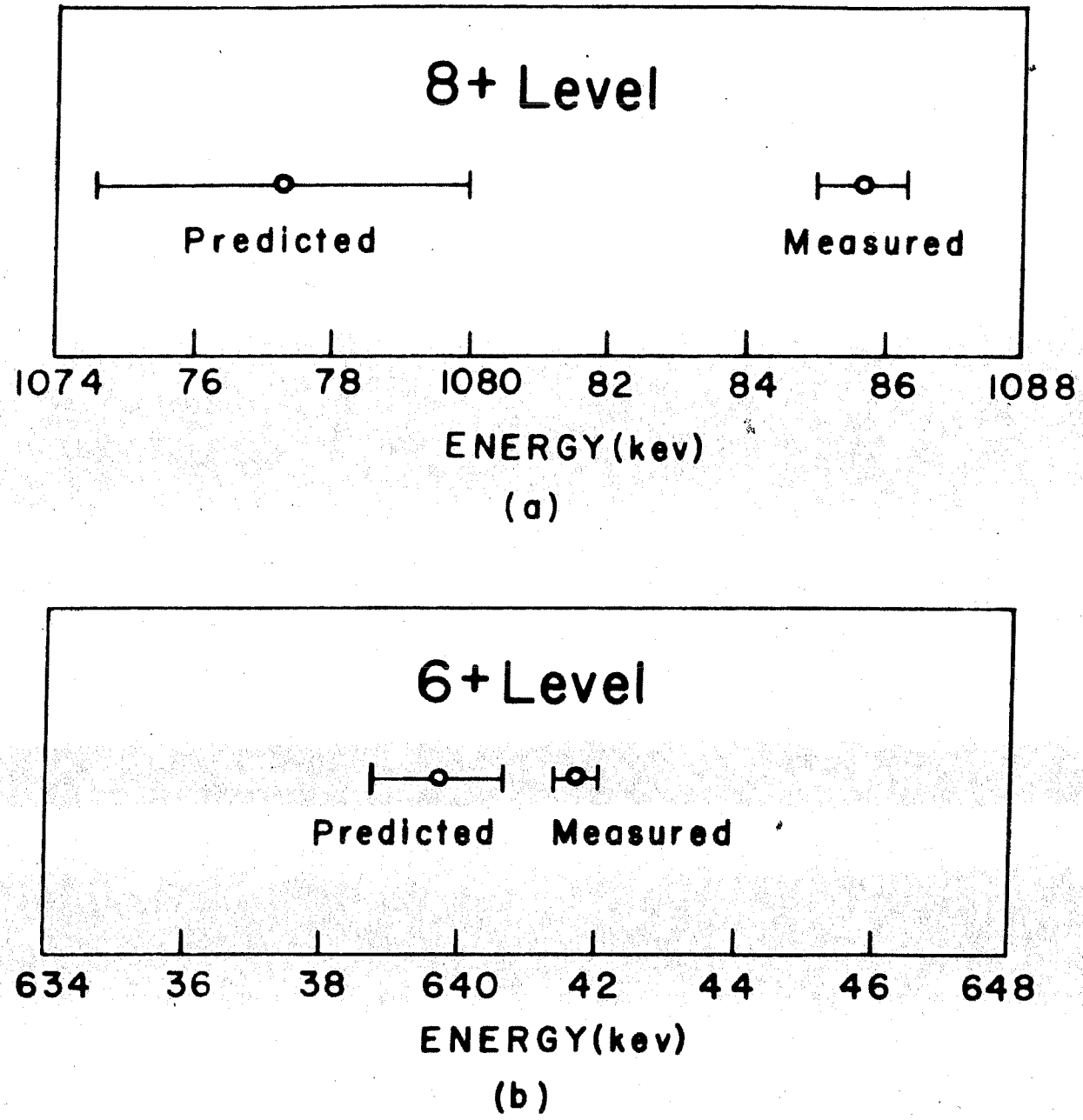

Figure 16. The deviations from the experimental values of the energies predicted by the two parameter formula for the 6+ and 8+ levels in Hf^{180}. The uncertainties represent 90% confidence limits.

APPENDIX II

THE DECAY OF Se^{75}

The Se^{75} electron capture to As^{75} decay scheme has until recently been in considerable doubt. The spin and parity assignments made in connection with a proposed decay scheme by Schardt and Welker (45) were later shown to be questionable. Pointing out some of the difficulties, Schardt (46) later proposed spin and parity assignments which have recently been well established.

A great weight of evidence has come from a number of research groups. Grigorev et al. (30) investigated the conversion coefficients of all of the transitions. Metzger and Todd (31) measured the conversion coefficients of the 401-, 305-, 279-, 136-, and 121-kev transitions. Van den Bold et al. (47) performed angular correlation experiments. A preliminary report was also given in connection with this study (48). All of the investigations have come to basically the same conclusions respecting the decay scheme. Except for a few weak high energy transitions, which have been reported by Bashilov and Il'in (49), the decay scheme is as shown in Fig. 17.

Transition energies measured here are listed in Table IX along with conversion coefficient information. Transition energies determine levels at the following energies (in kev): 198.60 ± 0.04, 264.66 ± 0.04, 279.53 ± 0.04, 303.91 ± 0.04, 400.65 ± 0.04. The conversion coefficients were normalized to the best fit of the 121.12-kev and 135.99-kev K-conversion coefficients to the theoretical E1 values. Their agreement with the theoretical values is shown in Fig. 18. The 24.3-kev gamma ray was not detected. Using a thin window NaI(Tl) scintillation spectrometer,

its upper limit was estimated to be 1/5 the intensity of the 66.05-kev gamma ray. A 24.3-kev M2 transition has a theoretical K-conversion coefficient of 160. From this and the known ratio of K-conversion electrons, the expected relative intensity is 1/50, so it is not surprising that the gamma ray was not observed. The K/L/M ratios agree with an M2 assignment.

The decay fractions of the transitions indicate weak beta branching to some of the excited levels. With the decay fractions normalized to 100%, assuming no primary beta branching to the ground-state, the feeding of the 264.62-kev level appears to be (2.9 ± 1.1)%. There is also some feeding, of the order of one or two percent, to either the 279.53-kev level or the 303.91-kev level or both. Because the gamma-ray intensity of the 24.3-kev transition connecting these levels was not found and the electron intensity of the transition was very uncertain, the ratio of the feeding of the two levels remains a question. According to the present spin assignments, the beta-transition to the 303.91-kev level is 2nd forbidden while that to the 279.53 ± 0.04 level is 1st forbidden, so branching to the latter is considered to be most likely.

One point that was still open to discussion was the mixing ratio of the 279.57-kev transition. Metzger and Todd, and later Manning and Rogers (50) have commented upon the disagreement between the mixing parameters, δ_1, as determined by conversion coefficient information and those determined by angular correlation. Table X lists the various mixing parameters as reported by the various groups or as calculated from their results. If Metzger and Todd's value is corrected to make the relative intensity of the 279.57-kev transition equal to 42 rather than 47 (as discussed on page 34) then the agreement between the conversion coefficient groups is rather good. The reported angular

correlation results of Van den Bold et al. (47) do seem to disagree with the other results, however, by plotting their a_2 coefficient on the theoretical curve of a_2 as a function of δ_1, agreement can be obtained.

The angular correlation coefficient a_2 in

$$W(\theta) = 1 + a_2 P_2(\cos\theta) \qquad (16)$$

is for the spin and multipole assignments for this transition given by

$$a_2 = (0.16 + 0.811\delta, + 0.082\ \delta_1^2)/(1 + \delta_1^2). \qquad (17)$$

This function is shown in Fig. 19. It appears, by plotting the a_2 coefficient of Van den Bold et. al. that they were somewhat optimistic in reporting the error on δ_1. Indeed, if one plots all of the a_2 coefficients reported by angular correlation and the mean of the δ_1 parameters calculated from conversion coefficients, the overlap of errors is seen to be reasonable as shown in Fig. 19.

If the value of 0.52 ± 0.10, which is the mean of the conversion coefficient measurements, is substituted into the expression relating the a_2 coefficient to δ_1, taking the sign of δ_1 as reported by angular correlation, the value of a_2 of $.44\ ^{+.02}_{-.04}$ is obtained which is within the reported errors for the a_2 coefficient as given by each angular correlation group.

It is the present conclusion that there is no great disagreement between the measurements of the mixing ratios of the 279.57 transition. Mean values, computed by weighting the conversion coefficient data according to the errors reported in the conversion coefficients (neglecting Metzger's original value) and weighting the angular correlation data according to the errors reported in the original a_2 coefficients, are from angular correlation $\bar{\delta}_1 = -0.52\ ^{+.06}_{-.11}$ and from internal

conversion coefficients $\overline{|\delta_1|} = 0.55 \pm 0.06$ which give a "best" mixing ratio for the transition of (78 ± 3) % M 1 + (22 ∓ 3)% E 2.

TABLE IX. Data for transitions in As^{75}

Gamma-ray energy (kev)	Gamma-ray relative intensity	Internal Conversion Coefficients α_K [a]	$K/(L+M)$	α_{total}	$\frac{\alpha_{K\ measured}}{\alpha_{K\ theoretical}}$ [b]	Multipolarity assignment	Decay fraction (percent) [c]
24.3	<0.3	-	d	-	-	(M2)	-
66.05 ± 0.01	1.63 ± 0.06	0.36 ± 0.05	e	0.42	-	M1 + E2	1.4 ± 0.1
96.74 ± 0.01	5.57 ± 0.18	0.81 ± 0.07	6.5	0.95	1.10 ± 0.10	E2	6.5 ± 0.3
121.12 ± 0.01	28.0 ± 0.6	(0.0406)[a]	10.5	0.0445	(1.10)[a]	E1	17.4 ± 0.4
135.99 ± 0.02	95.5 ± 1.8	(0.0240)[a]	7.6	0.0272	(0.91)[a]	E1	58.5 ± 1.1
198.60 ± 0.06	2.4 ± 0.1	0.018 ± 0.002	-	0.018	-	M1 + E2	1.5 ± 0.1
264.62 ± 0.07	100	0.0060 ± 0.0005	9.5	0.0067	0.97 ± 0.08	M1	60.1
279.57 ± 0.08	42.2 ± 0.6	0.0076 ± 0.0009	7.9	0.0086	-	M1 + E2	25.4 ± 0.4
304.0 ± 0.3	2.29 ± 0.14	0.045 ± 0.006	6.1	0.052	0.99 ± 0.13	E3	1.4 ± 0.1
400.7 ± 0.2	19.5 ± 0.6	0.0011 ± 0.0001	8.8	0.0012	0.94 ± 0.09	E1	11.6 ± 0.4

a. The conversion coefficients were normalized to the best fit of the coefficients of the 121.12-kev and 135.99-kev transitions with theoretical E1 values.

b. The theoretical coefficients are those given by Rose (6) based upon the multipolarity assignments in column 7.

c. The decay fraction is proportional to $(1 + \alpha_{total})$ and is normalized to 100% feeding of the ground state neglecting any beta branching to that level.

d. K/L/M = 3.7/1/0.24.

e. K/L/M = 8.3/1/0.02.

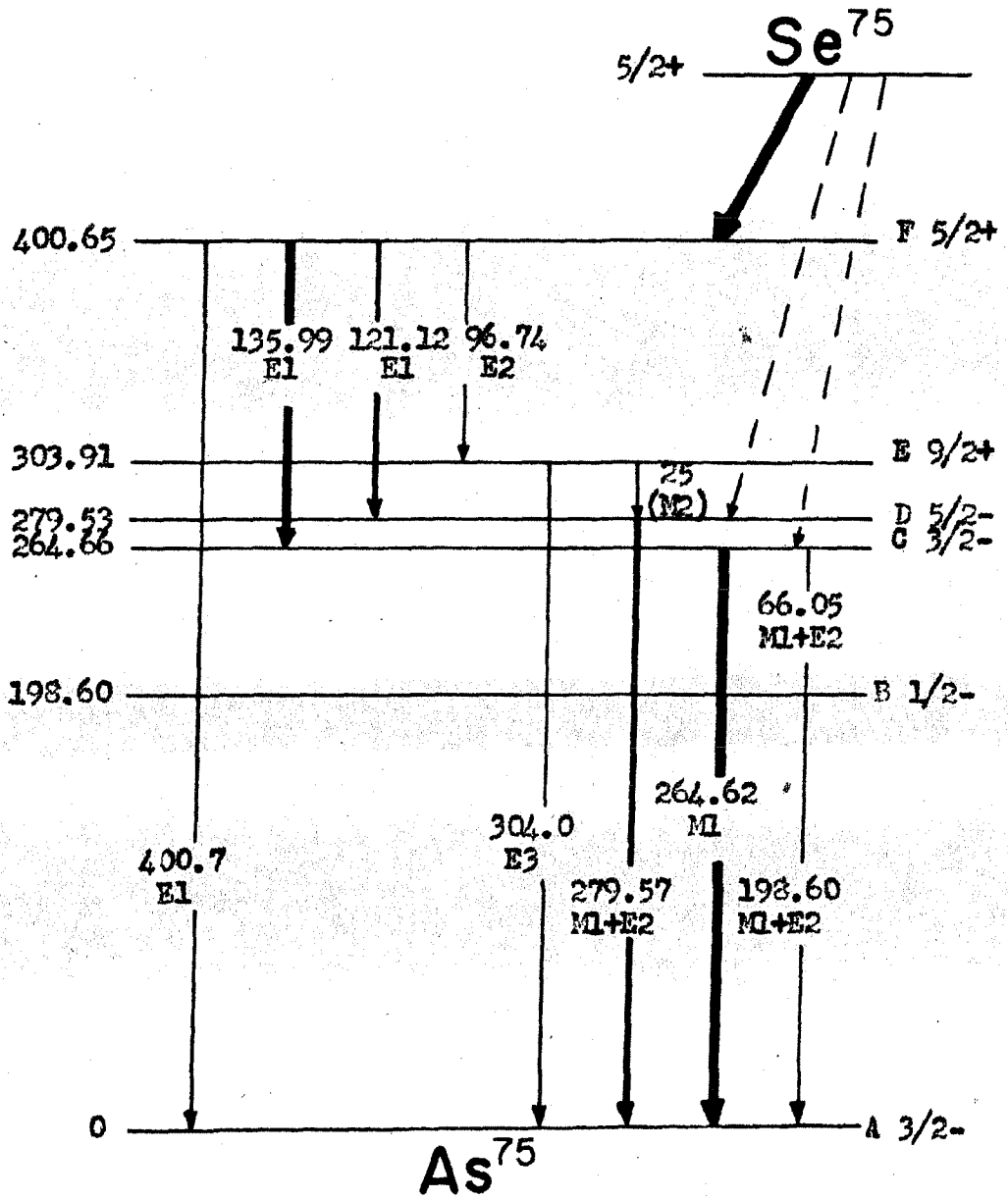

Figure 17. The Decay Scheme of Se^{75}.

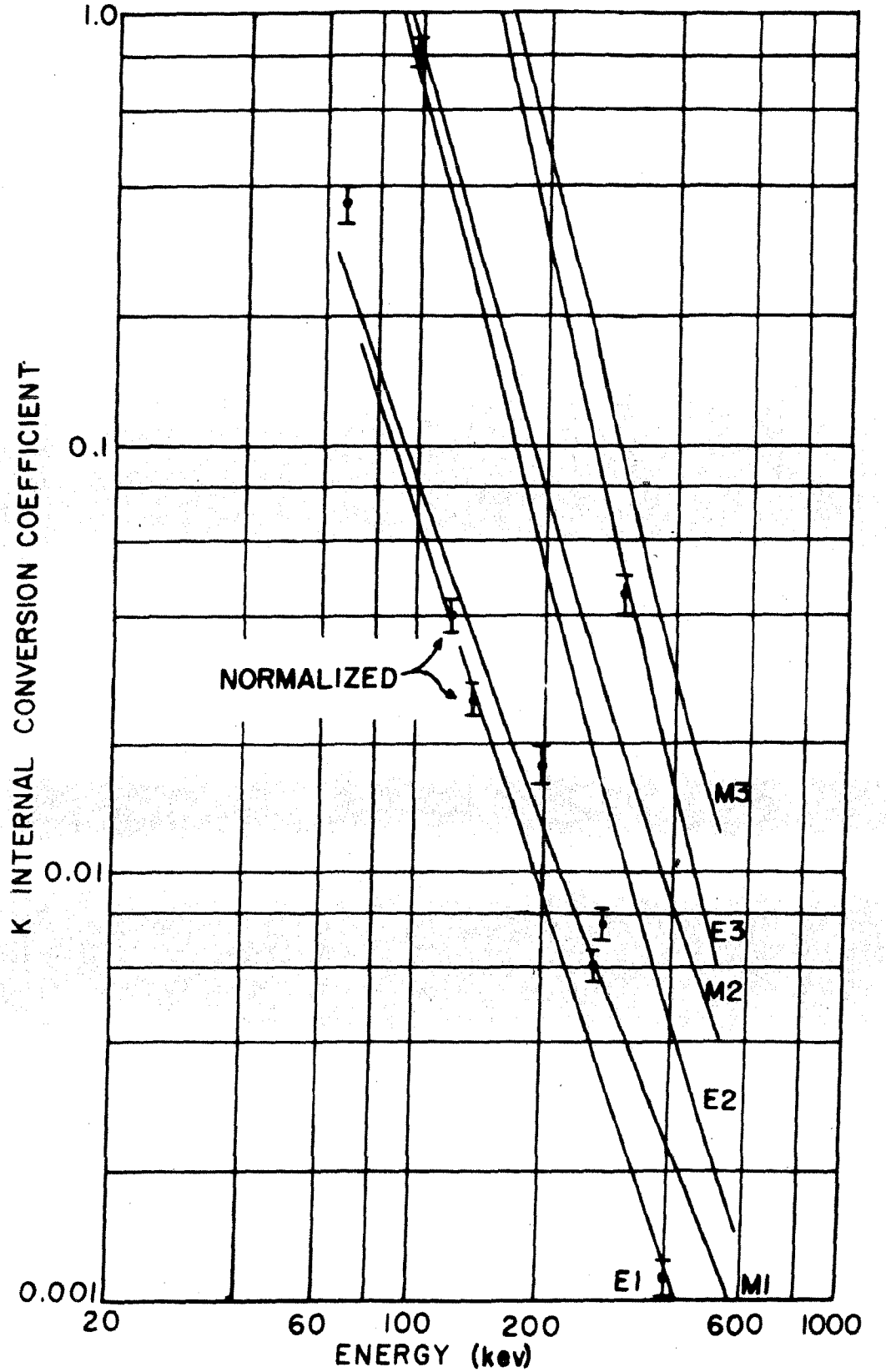

Figure 18. K-conversion coefficients of transitions in As^{75}. The curves are the theoretical values of Rose (31). The measured coefficients are normalized to a "best" fit of the 121.12-kev and 135.99-kev transitions to theoretical E1 values.

TABLE X. Mixing parameter, δ, for the 279.57-kev transition in As^{75}

By internal conversion

Author	a_K	$\lvert\delta\rvert$
Metzger and Todd (31)	8.0 ± 0.5[a]	0.58 ± 0.08
Grigorev et al. (30)	7.6 ± 0.8	0.52 ± 0.12
Bashilov and Il'in (49)	7.6 ± 1.0	0.52 ± 0.16
Present Worker	7.6 ± 0.9	0.52 ± 0.14

By angular correlation[b]

Researcher	a_2	δ
Schardt and Welker (45)	-0.42 ± 0.03	(-0.44 ± 0.11)
Kelly and Wiedenbeck (51)	-0.41 ± 0.03	(-0.41 ± 0.08)
Van den Bold et al. (47)	-0.466 ± 0.02	(-0.75 ± 0.21)[c]

a. The reported value by Metzer and Todd has been corrected for the present "best fit" gamma intensity.

b. Brackets indicate that the value of δ has been deduced from the reported a_2 coefficient.

c. The value deduced from the a_2 coefficient is given. Van den Bold et al., however, report $\delta = \mp 0.75 \pm 0.10$. For a discussion of this discrepancy see p. 83.

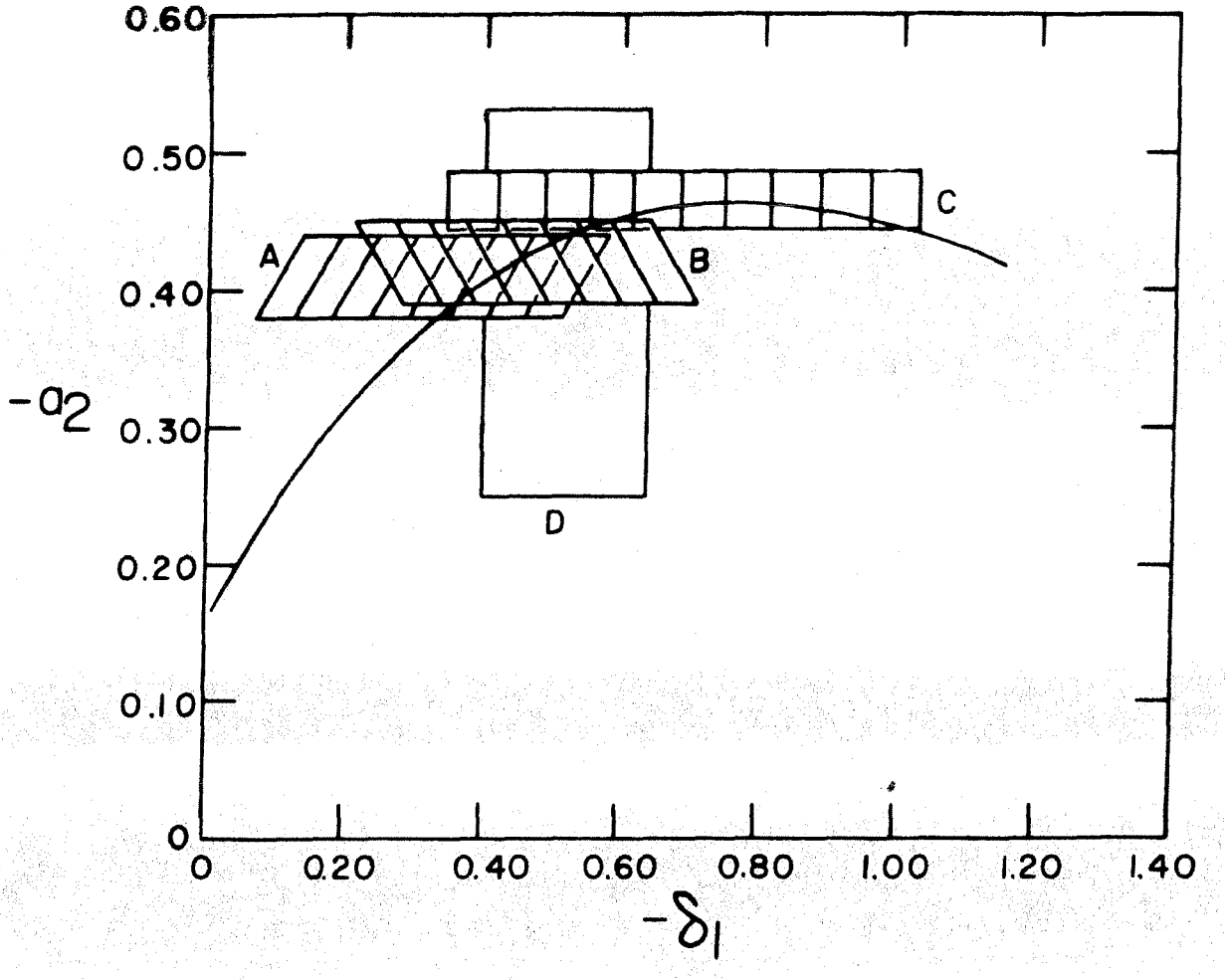

Figure 19. The a_2 coefficient as a function of the mixing parameter of the 279.57-kev M1 + E2 transition in As^{75}. A, B, and C, show the experimental a_2 coefficients measured by Kelly and Widenbeck (41), Schardt and Welker (37) and Van den Bold, et al. (42). The mixing parameters corresponding to these measurements may be found from the theoretical curve. D gives a mean of the conversion coefficient determinations of various authors. See pp. 82-84 and Table X.

APPENDIX III

W^{187} ENERGIES AND DECAY SCHEME

Introduction

Much information has been gathered on the beta decay of W^{187} into Re^{187} and a number of disintegration schemes have been proposed (38) (52) (53). Certain aspects of the scheme are agreed upon by all of the investigators. The series of levels appearing near the energies 134-kev, 206 kev, and 686 kev are well attested by gamma cascade transitions with abundant crossovers to check the energies. In addition, the 134-kev level has been coulomb excited so its position is well verified.

Gamma-ray Energies

Five of the gamma-rays were previously measured by Muller et al. using the curved-crystal spectrometer. They found the following energies: 686.1, 618.9, 479.5, 134.25, and 72.00 kev (54).

Two of the lines reported by Muller et al. have been remeasured with the resulting energies being 479.4 ± 0.4 and 618.2 ± 0.6. In addition, ten of the weaker transitions have been detected with the curved-crystal spectrometer yielding, in addition to the three lines previously measured, the gamma-ray energies listed in Table VI. Fig. 20 shows the only lines not completely resolved with the curved-crystal spectrometer and their decomposition. These are the 617.2-kev and 625.1-kev gamma rays.

The basic level structure as previously reported is confirmed. These levels are at 134.25, 206.25, and 686.1 kev as shown in Fig. 21. (In cases where the limits of error on the sum or difference of two

gamma-ray energies is of the order of that on the energy of the cross-over transition, the level energy indicated is the weighted mean.) In addition, there is a set of levels with energies 511.6, 618.2, 625.1, and 864.5 kev above a fundamental level which are established as a unit by the following gamma rays: 618.2, 625.1, 511.3, 113.74, 106.61, 239.3, 246.3, and 867 kev. There is no reason from the energies, to assign these as feeding the ground state. By coincidence measurements, however, Gallagher, Edwards, and Manning (34) have shown that the 625.1- and 618.2-kev gamma rays do not feed the 134.25-kev state or the 206.25-kev state, in contradiction to the results of Dubey (53). They also found that the difference in energy between the ground states of W^{187} and Re^{187} is 1308 $\pm$ 10 kev which precludes having this group feed the 686-kev state. Because of the coincidence measurements and the available energy, the group was assigned to feed the ground state.

The 773-kev transition is assigned to feed the ground state, in agreement with Vergnes, again because of the gamma-gamma coincidence measurements of Gallagher et al. and energy considerations.

Multipolarity Assignments

The transition multipolarity assignments are given in Table VI. They are based upon the absolute conversion coefficients discussed in section IV B.

Spin and Parity Assignments

Whereas the multipolarities of the transitions and the energies of the levels seem unambiguous, this is not the case with the spin and parity assignments. It is clear, however, that the multipolarity assignments are completely consistent with the level scheme as given in Fig. 21. No crossover transition, for instance, contradicts the parities of two

levels as determined by the cascade gamma rays.

In the assignment of spins and parities, the ground state spin of Re^{187} was taken to be 5/2+. The 134.25-kev state has been Coulomb excited (55) and the 7/2+ assignment seems entirely consistent with an expected rotational state. The 206.25-kev state spin assignment of 9/2- has also been previously reported and seems to be firm. Only a 5/2- spin assignment for the 686.1-kev state is consistent with the spins of the ground state, the 134.25-kev state, the 206.25-kev state, and the transitions connecting these with the 686.1 kev state.

The spins and parities of the group of levels 511.6, 618.2, 625.3, and 864.5 kev are related by the eight transitions connecting these levels and the ground state. Two mutually exclusive sets of spins may be assigned to these levels. Both are given in Fig. 21. The set of lower spins is preferred because transitions to the 134.25-kev level are not observed.

A ground state spin and parity of 3/2- can be assigned to W^{187} which is consistent with the spin and parity assignments in the levels of Re^{187} and the observed branching to these levels. Table XI gives the branching ratios and log ft values for these transitions. With the exception of the ground state branching which was taken to be 20% from the results of Cork et al. (52) and Dubey et al. (53), the branching ratios were calculated from the decay fractions of the electromagnetic transitions.

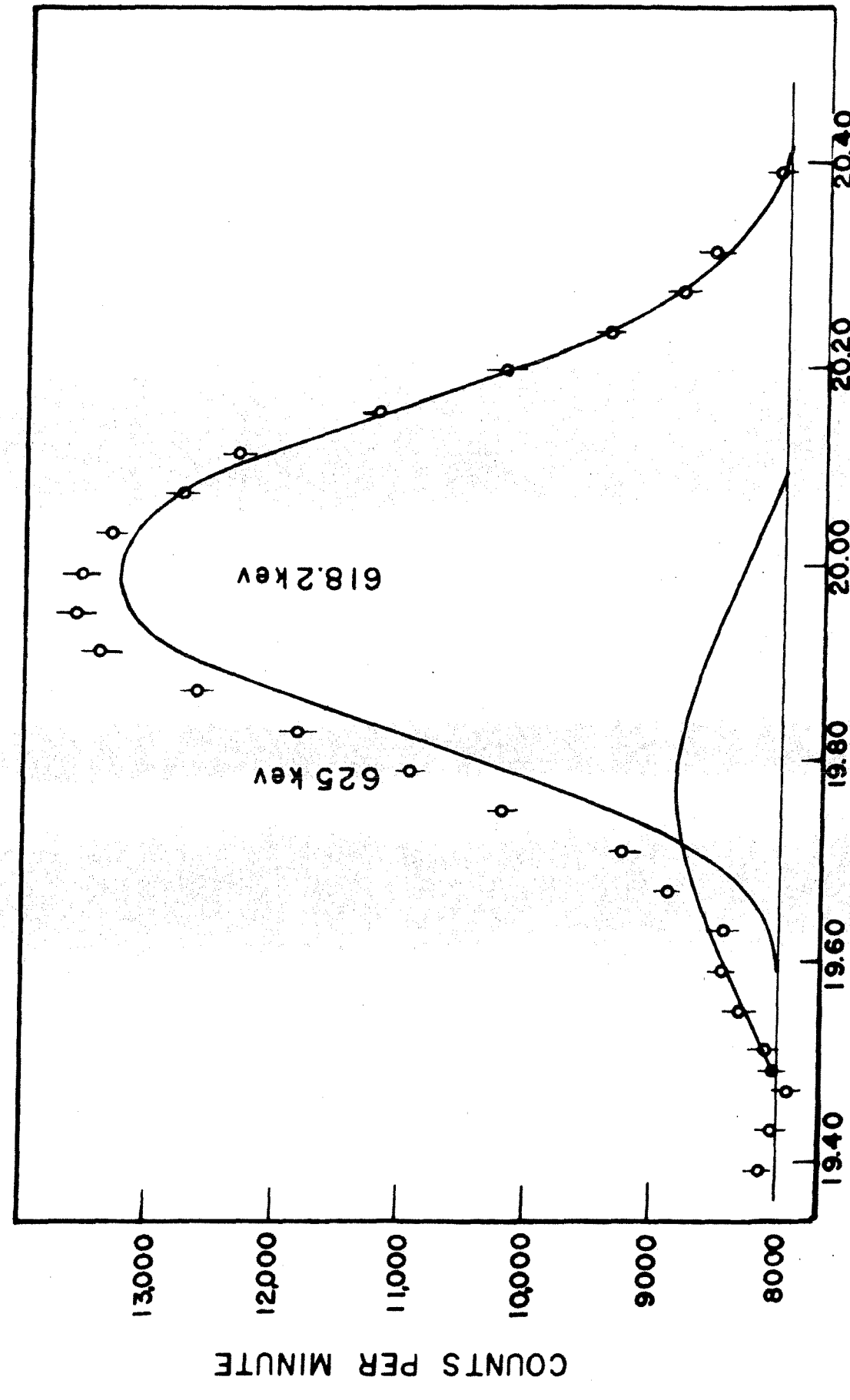

Figure 20. A portion of the gamma-ray spectrum from the decay of W^{187} as measured with the curved-crystal spectrometer. The decomposition into the 618.2-kev and 625-kev gamma rays is shown.

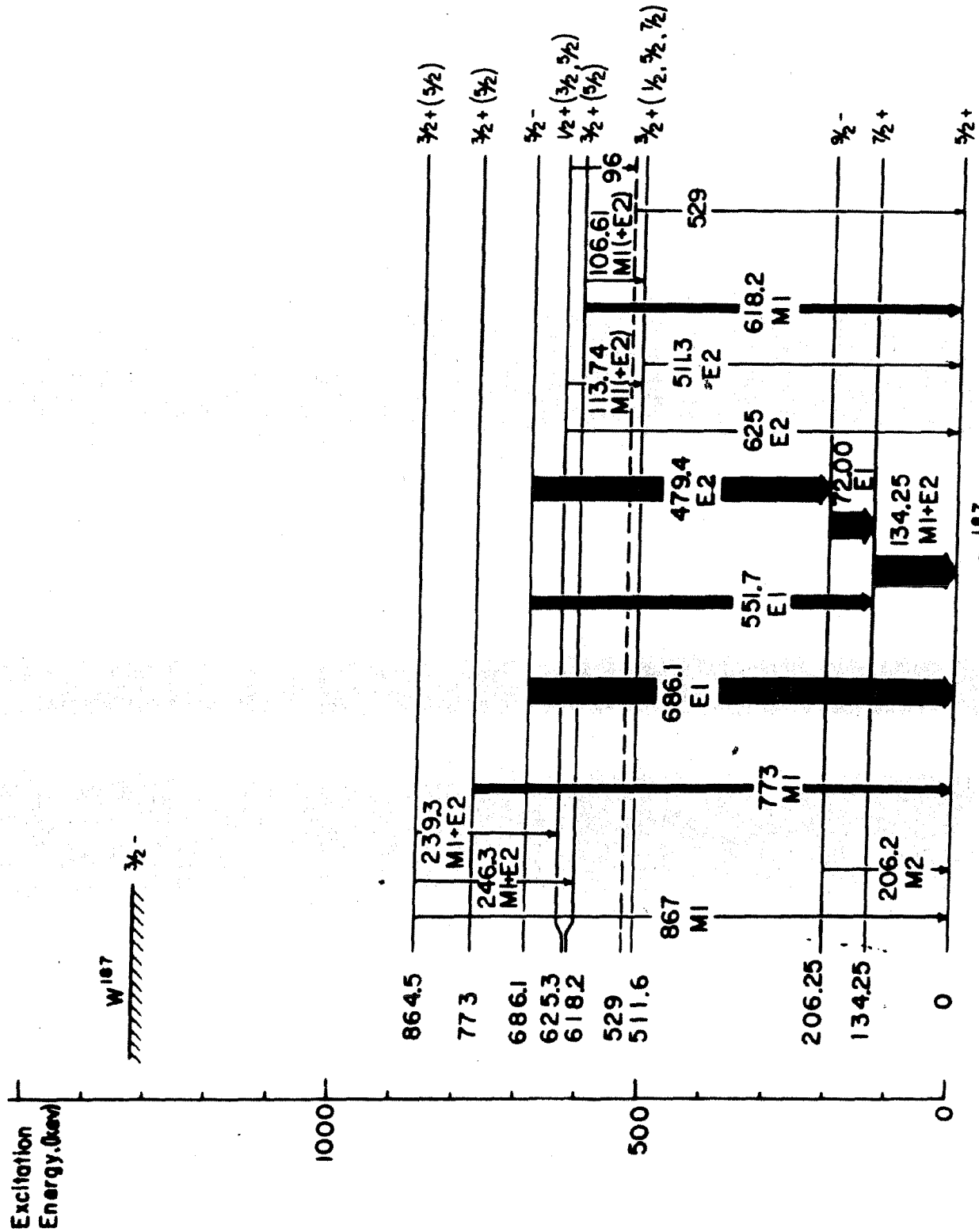

Figure 21. The decay scheme of W^{187}.

TABLE XI. Beta decay branching and log ft values for $W^{187} \rightarrow Re^{187}$

Level energy (kev)	Beta transition energy (kev)	Primary beta branching (percent)[a]	Log (ft)
0	1308	(20)[a]	7.9
511.6	796	$\leq$0.38	$\geq$9.0
618.2	690	4.0	7.7
625.3	683	6.7	7.4
686.1	622	64	6.3
773	535	4.1	7.3
864.5	444	~0.7	~7.8

a. In calculating the primary branching to the upper states, the sum of the intensities of the electromagnetic transitions feeding the ground state was set equal to 80% of the total primary beta branching. This is consistent with the ground-state branching ratio reported by Cork et al. (52) and Dubey et al. (53).

APPENDIX IV

CURVED-CRYSTAL SPECTROMETER INTENSITY THEORY

It is well known that the lifetimes of x rays and gamma rays differ considerably. X-ray lifetimes are of the order of 10^{-14} sec while those of gamma rays are usually considerably longer--of the order of 10^{-9} sec and longer. According to the uncertainty principle, this means that the energy uncertainty, or the natural line width, of an x ray will be some 10^5 times the uncertainty of a gamma ray. X rays in the high Z region, whose energies are of the order of tens of kilovolts, have natural line widths of the order of electron volts. The line shape of W $K\alpha_1$ on a wavelength scale has a full-width at half-maximum, as observed by Barnes and Palmer (reported in Compton and Allison (56)), of 0.150 xu. This corresponds to an energy width of 43 ev.

The instrument window profile of the gamma-ray spectrometer has a full-width of approximately 0.28 xu. Thus, the natural width of the x ray is of the order of the width of the instrument window while the natural width of a gamma-ray line is very small compared with the instrument window. Because of this, it is difficult to put x-ray and gamma-ray intensities on the same scale. Before proceeding with this problem, a general approach to intensity measurements will be given.

General

The recorded line is the fold of the spectral line profile into the instrument window profile. A particular spectral line can be described by a function $f_i(x)$ where $x = \lambda - \lambda_i$, λ being the wavelength and λ_i the wavelength of the center of the line. The instrument window

is a function of its center position as well as of the distance from the center position y. (The discussion that follows is not dependent upon any symmetry properties of either the spectral line or the instrument window profile. For non-symmetrical lines, "center" should be given any convenient, reproducible definition.) There are many lines, f_1, f_2, ... but only one instrument window g. For a particular spectral line, the observed profile $F_i(x, \lambda_i)$ is the fold of the instrument window into the spectral line;

$$F_i(x, \lambda_i) = \int_{-\infty}^{\infty} f_i(\xi)g(x-\xi, \lambda_i+x)d\xi \quad . \tag{18}$$

If the instrument window profile does not change significantly as its center position is swept over the spectral line, then $g(y, \lambda_i + x) \approx g(y, \lambda_i)$ and Eq.(18) becomes

$$F_i(x, \lambda_i) = \int_{-\infty}^{\infty} f_i(\xi)g(x-\xi, \lambda_i)d\xi \quad . \tag{19}$$

The integral of the observed line is

$$\int_{-\infty}^{\infty} F_i(x, \lambda_i)dx = \int_{-\infty}^{\infty}\int_{-\infty}^{\infty} f_i(\xi)g(x-\xi, \lambda_i)\, d\xi\, dx. \tag{20}$$

Changing the order of integration this becomes

$$\int_{-\infty}^{\infty} F_i(x, \lambda_i)dx = \int_{-\infty}^{\infty} f(\xi)\left[\int_{-\infty}^{\infty} g(x-\xi, \lambda_i+x)dx\right] d\xi \tag{21}$$

$$= \int_{-\infty}^{\infty} f(\xi)d\xi \int_{-\infty}^{\infty} g(x, \lambda_i)dx. \tag{22}$$

The intensity of the line, I, is defined as

$$I_i = \int_{-\infty}^{\infty} f_i(x)dx = \int_{-\infty}^{\infty} F_i(x, \lambda_i)dx \Big/ \int_{-\infty}^{\infty} g(x, \lambda_i)dx \tag{23}$$

The relative intensity of two lines is

$$I_1/I_2 = \left[\int_{-\infty}^{\infty} F_1(x,\lambda_1)dx \Big/ \int_{-\infty}^{\infty} F_2(x, \lambda_2)dx\right]\left[\int_{-\infty}^{\infty} g(x, \lambda_2)dx \Big/ \int_{-\infty}^{\infty} g(x, \lambda_1)dx\right] \tag{24}$$

The quantity $\int_{-\infty}^{\infty} g(x, \lambda_i)dx$ is called the integrated reflection coefficient. Lind, West, and DuMond (27) give an expression for the integrated

reflection coefficient as derived theoretically for a curved mosaic crystal with low primary and secondary extinction from which the following ratio, R_{12}, is obtained

$$R_{12} = \int_{-\infty}^{\infty} g(x, \lambda_2)dx \Big/ \int_{-\infty}^{\infty} g(x, \lambda_1)dx = (\lambda_2/\lambda_1)^2 \qquad (25)$$

This relationship has been confirmed within the limitations stated in the next section. Therefore, for any two lines, regardless of width or shape, the relative intensity is equal to the ratio of the integrals of the observed lines times R_{ij}.

Peak Height Measurements

If the line is very narrow compared with the instrument window, as is certainly the case with gamma rays, then $f_i(x) = I_i \delta(x)$ and the observed line shape given by Eq. (19) becomes

$$F_i(x, \lambda_i) = I_i g(x, \lambda_i) \ . \qquad (26)$$

Thus it is seen that under these conditions, the recorded profile will have the same shape as the instrument window.

In measuring gamma rays, it has been observed that the intensity, but not the shape, of the instrument window profile changes as a function of the center position wavelength;

$$g(x, \lambda_1) = h(\lambda_1, \lambda_2) g(x, \lambda_2) \ . \qquad (27)$$

The quantity $h(\lambda_1, \lambda_2)$ is equal to the ratio R_{12} as defined in Eq. (25) and hence for corresponding points, x, on the observed spectral line

$$I_1/I_2 = \left[F_1(x, \lambda_1)/F_2(x, \lambda_2)\right] R_{12} = \left[F_1(x, \lambda_1)/F_2(x, \lambda_2)\right] \ (\lambda_2/\lambda_1)^2$$

The ratio of the observed profile heights at any fiducial point is thus seen to be equal to the ratio of the profile integral, and this means that the ratio of these heights can equally well be used as the ratio of the integrals for the determination of the intensity ratio of the

two lines. Obviously, the most suitable fiducial point is the peak of the line ($x = 0$).

If the window shape were not invariant, the same general theory would still apply for any choice of the fiducial point x_f. The only change in the above formulae would be that $h(\lambda_1, \lambda_2)$ would now also depend on the choice of this fiducial point. Then the ratio $h(\lambda_1, \lambda_2, x_f)$ might be different from the ratio $R_{12} = (\lambda_2/\lambda_1)^2$ of the integrated reflection coefficient.

This means that what has really been determined in the intensity calibration of Part III is the quantity $h(\lambda_2, \lambda_1, 0)$ which might be called the "peak reflection coefficient" ratio and which is equal to the "integrated reflection coefficient" ratio as defined by Lind et al. (26) under the assumption that the instrumental window has an invariant shape on a wavelength scale.

It might be of interest to study with greater precision whether the assumption of an invariant window shape is justified. Whether or not this is the case, however, does not impair the usefulness of the present intensity calibration, based on the peak heights, as long as it is applied to lines with a negligible natural width.

Extension of Intensity Scale to Lines with a Non-negligible Natural Width

The above peak height scale does not apply to the case of an x-ray line with a non-negligible natural width. Still, Eq. (24) holds, and we can obtain an intensity figure by integrating the observed line profile.

This integration process is in practice difficult to perform because the natural shape of an x-ray line is very close to that of a resonance curve ("witch")

$$f(x) = A(1 + x^2/a^2)^{-1} \qquad (28)$$

where 2a is the full-width at half-maximum. This function has the unfortunate property of approaching zero very slowly. At 1.5 full-widths from the center of the line, the function is still equal to 10% of the peak value. The area under the tails beyond this point is a full 20% of the total area.

Of course, the function that will actually be integrated is the fold of the instrument window and the resonance curve which does not behave quite so badly. It still drops off like $1/x^2$ in the tails, but for an x-ray line of full-width 0.15 xu, only about 8.5% of the area remains in the tails of the composite line after integrating to 1.5 full-widths. Fig. (22) shows the instrument window profile and a witch for comparison.

To compare x-ray intensities, no great problem is involved, for if the natural line widths do not differ too greatly, one can integrate out to a convenient point and stop. If the amount left in the tails is small, then the error in relative x-ray intensities will be second order and about the same fraction is neglected in each line. When comparing an x ray and a gamma ray, however, the integration of the gamma ray is just the integration of the instrument window which goes to zero very rapidly, so any area left unintegrated in the x ray would now be a first-order correction to the relative intensity. This problem arose in the present study in connection with the normalization of the conversion coefficients in the W^{187} decay.

Integration of the Observed Line Profile

For the integration of an observed x-ray peak, the first problem that arises is how to separate the tail from the background. In the case studied here, the problem was solved by observing the output

pulses from the detector with a 100-channel pulse height analyzer. Even at four full-widths from the center of the diffraction peak, the spectrum from the scintillation counter clearly showed a photopeak at the correct energy. Fig. 23 shows the W Kα x ray as observed with the spectrometer. The statistical uncertainty on every point except the one at 211.70 Screw Division is better than 1%, while the last point in the tail has 2% statistical uncertainty. The background has been subtracted from all points. The curve, with the scale expanded by a factor of 10, is given starting at 210.40 S.D. showing that the tail is still falling off in a very smooth manner.

Fig. 22 shows a similar run over a gamma-ray line at approximately the same energy. At slightly more than one full-width, no counts in the line could be detected. This represents the instrument window. The full-width of the instrument window in this case is 0.280 S.D. while the x-ray composite peak has a full-width of 0.378 S.D.

An integration of the two lines was performed in the following manner. The gamma ray was integrated with a planimeter. The x-ray composite line was integrated in the same manner to 1.5 full-widths; then, using the expanded scale, the integration was extended to 4.2 full-widths. It can be shown that the fold of any window, of finite extension in λ, into a witch will leave tails which correspond to another witch. A theoretical witch, whose full-width corresponds to the reported natural line width of W $K\alpha_1$ (0.150 xu), was therefore fitted to the tails of the experimental curve. This curve is shown in the expanded scale beside the measured curve. The theoretical witch thus fitted was then analytically integrated to infinity. The area contributed by the tail beyond 1.5 full-widths was 8.5% of the total area.

The intensity ratio between the x ray and the gamma ray that was

found by this integration procedure connects the x ray to the intensity scale established for gamma rays from the observed peak heights. It turned out that the factor by which the peak height of this x ray should be multiplied to fit it to the peak height intensity scale for lines of negligible width is 1.62 ± 0.03.

Alternate Method

An alternate method for arriving at the correction factor mentioned above can be followed if the natural line-width of the x ray is known.

The ratio of the intensities of an x ray and a gamma ray is given by

$$I_X/I_\gamma = \int_{-\infty}^{\infty} f_x(y)dy/\int_{-\infty}^{\infty} f_2(y)dy \quad . \tag{29}$$

From Eq. (19) the counting rate at the peak of the observed line can be written

$$F_i(0, \lambda_i) = \int_{-\infty}^{\infty} f_i(\xi)g(-\xi, \lambda_i)d\xi \quad . \tag{30}$$

The intensity ratio can therefore be written as

$$I_x/I_\gamma = \left[\int_{-\infty}^{\infty} f_x(y)dy/\int_{-\infty}^{\infty} f_x(y)g(-y, \lambda_x)dy\right] \left[\int_{-\infty}^{\infty} f_\gamma(y)g(-y, \lambda_\gamma)dy/\int_{-\infty}^{\infty} f_\gamma(y)dy\right] \cdot F_x(0, \lambda_x)/F_\gamma(0, \lambda_\gamma) \quad . \tag{31}$$

The instrument window profile $g(-x, \lambda_i)$ can be found by measuring a line whose natural width is very small (a gamma ray for instance) and a plot of $g(-x, \lambda_x)/g(0, \lambda_x)$ may be made. If the natural line width of the x ray is known then the function $Bf_x(y)$ may be plotted assuming f to be a resonance curve as in Eq. (28) and B is a scale factor. By multiplying the two functions together point by point (not folding them) $Bf_x(y)g(-y,\lambda_x)/g(0, \lambda_i)$ is obtained. By measuring the areas of this composite curve and the x-ray resonance curve, the following ratio is

obtained,

$$r = \left[\int_{-\infty}^{\infty} f_x(y)dy \Big/ \int_{-\infty}^{\infty} f_x(y)g(-y, \lambda_x)dy\right] g(0, \lambda_i) \quad . \tag{32}$$

For a gamma ray where $f_\gamma = I_\gamma \delta(y)$,

$$\int_{-\infty}^{\infty} f_\gamma(y)g(-y, \lambda_\gamma)dy \Big/ \int_{-\infty}^{\infty} f_\gamma(y)dy = g(0, \lambda_\gamma) \quad . \tag{33}$$

Using Eqs. (32) and (33) the x-ray to gamma-ray intensity ratio given in Eq. (31) becomes

$$I_x/I_\gamma = \left[F_x(0, \lambda_x)/F_\gamma(0, \lambda_\gamma)\right]\left[g(0, \lambda_\gamma)/g(0, \lambda_x)\right] r \quad . \tag{34}$$

The quantity $g(0, \lambda_\gamma)/g(0, \lambda_x)$ is just the peak reflection coefficient ratio $h(\lambda_\gamma, \lambda_x, 0)$. The quantity r is therefore the factor by which the x-ray peak height intensity must be multiplied to connect it with the gamma-ray peak height intensity scale.

In this procedure, there are no difficult folds to perform graphically. Only one relatively simple graphical multiplication of functions and the integration of the resulting curve is necessary. Where r has been deduced by other methods such as that given in the last section, this procedure might be used to obtain the width of the x-ray line. Fig. 22 shows the application of this procedure to W $K\alpha_1$. The x ray full-width used was 0.150 xu as reported by Barnes and Palmer and given in reference (56). The value of r obtained is 1.6 which agrees well with the value 1.62 obtained by the former method which implies that the natural width for the K-α, x rays of Re and W is very similar.

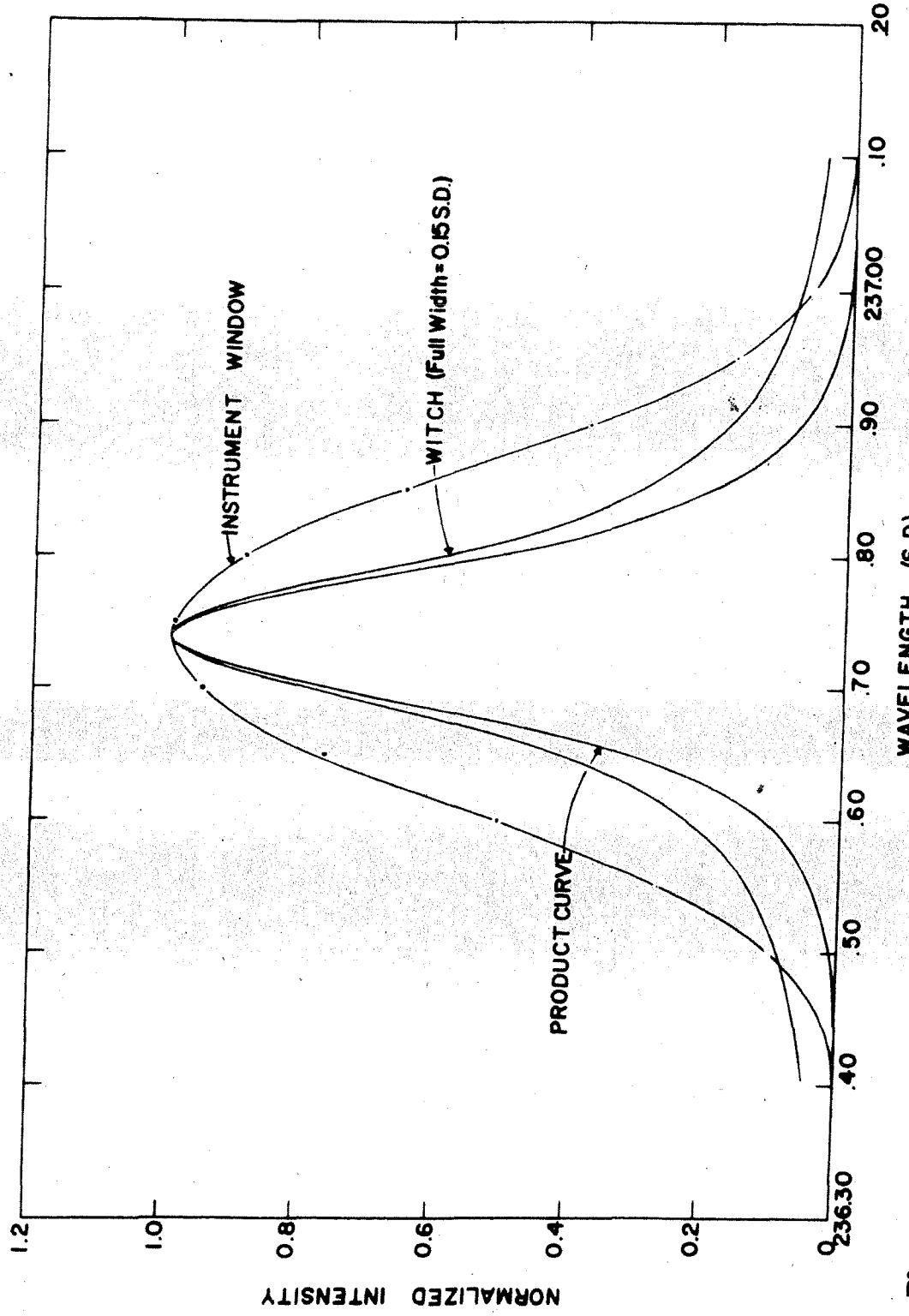

Figure 22. The instrument window profile of the curved-crystal spectrometer found by measuring the 52.57-kev gamma-ray in W^{183}. The product curve (not a fold) was found by multiplying the ordinate values of the instrument window with a resonance curve (witch) having a full-width at half-maximum of 0.15 S.D. Statistical uncertainties of the points on the instrument window curve are indicated by the size of the points.

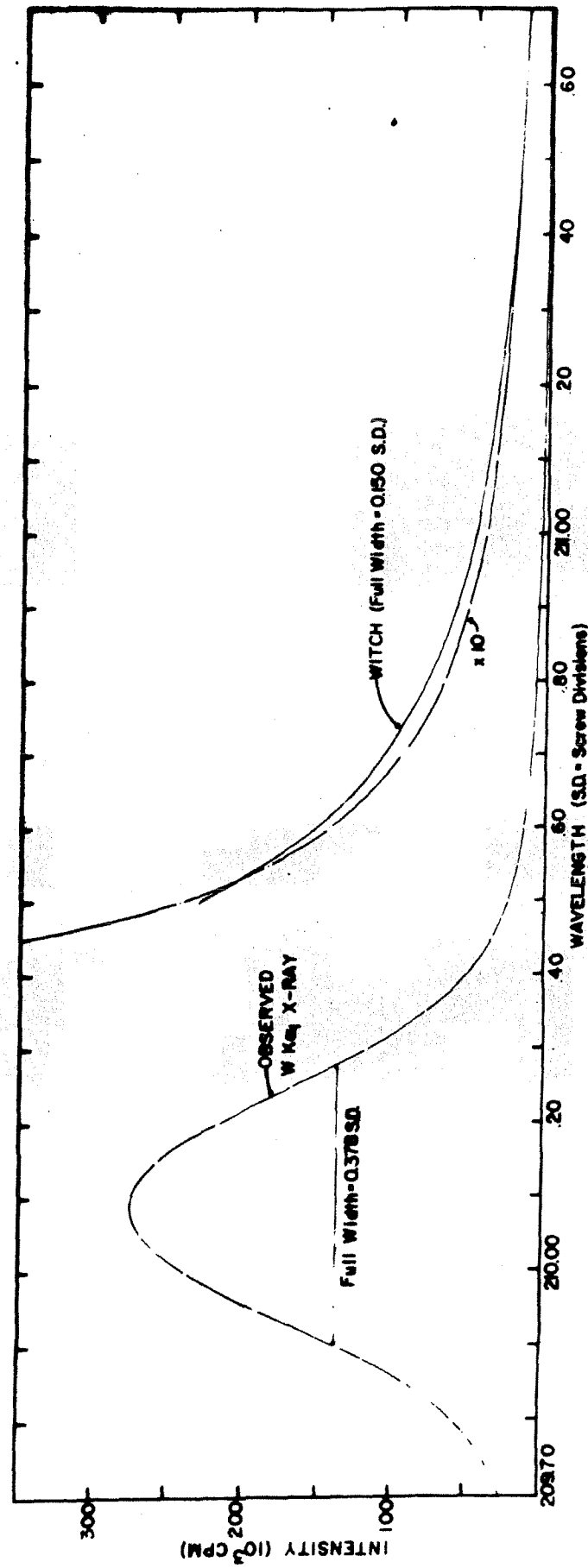

Figure 23. W K x ray measured with the curved-crystal spectrometer. The "Screw Division" (S.D.) is an instrument unit and is equal to $\pi/1.00055$ plus a constant (approximately 1 mm). The measured curve above 210.45 S.D. is also shown with the ordinate expanded by a factor of 10. Statistical uncertainty on all points except that at 211.70 S.D. is less than 1%. The latter point has a 2% uncertainty. The error is shown by the size of the experimental point.

References

1. Rose, Goertzel, Spinrad, Harr and Strong, Phy. Rev. 83 79 (1951).

2. A. H. Wapstra and G. J. Nijgh, Nuclear Phys. 1, 245 (1956).

3. L. A. Sliv, Zh. eksper. teor. Fiz, 21, 770 (1951).

4. L. A. Sliv and M. A. Listengarten, Zh. eksper. teor. Fiz., 22, 29 (1952).

5. L. A. Sliv and I. M. Band, Part I (K-shell conversion coefficients) and Part II (L-shell conversion coefficients), Acad. of Sciences, USSR (Moscow-Leningrad, 1956), issued in the USA as reports 57 ICC K1 and 58 ICC L1, Physics Dept., Univ. of Ill.

6. M. E. Rose, Internal Conversion Coefficients (North-Holland Publishing Co., Amsterdam, 1958).

7. E. L. Church and J. Weneser, Phys. Rev. 104, 1382 (1956).

8. T. A. Green and M. E. Rose, Phys. Rev. 110, 105 (1958).

9. L. S. Kisslinger, Phys. Rev. 114, 292 (1959).

10. Scharff-Goldhaber, McKeown, and Mihelich, Bull. Am. Phys. Soc. 1 no. 4 206 (1956).

11. S. G. Nilsson and J. O. Rasmussen, UCRL-3889, University of California (1957).

12. K. Siegbahn, β-ray Spectrometer Theory and Design, in Beta-and Gamma-Ray Spectroscopy, ed. K. Siegbahn, (North Holland Pub. Co., Amsterdam, (1955) p. 52.

13. J. J. Murray, F. Boehm, P. Marmier, and J. W. M. DuMond, Phys. Rev. 97, 1007 (1955).

14. J. W. M. DuMond, Crystal Diffraction Spectroscopy of Nuclear Gamma-rays, Ibid, p. 100.

15. J. W. M. DuMond, Ergebnisse d. exakt. Naturwiss, Bd XXVIII S. 232-301 (1955).

16. Cohen, DuMond, Layton, and Rollett, Rev. Mod. Phys. 27, 363 (1955).

17. J. W. M. DuMond, Annals of Physics 2, 283 (1957).

18. H. E. Henrickson, Report No. 24, USAEC, California Institute of Technology, 1956.

19. H. Slätis, Source and Window Technique, in Beta-and Gamma-ray Spectroscopy, op cit.

20. D. Strominger, J. M. Hollander, and G. T. Seaborg, Rev. Mod. Phys. 30, 585 (1958).

21. G. W. Grodstein, NBS Circular 583, U. S. Government Printing Office, Washington, (1957).

22. R. T. McGinnies, NBS Supplement to Circular 583, U. S. Government Printing Office, Washington, (1959).

23. M. J. Berger and J. Dogget, J. Research Natl. Bur. Standards, 56, 355 (1956).

24. A. H. Wapstra, G. J. Nijgh and R. Van Lieshout, Nuclear Spectroscopy Tables, (North-Holland Publishing Company, Amsterdam, 1959).

25. P. Axel, Rev. Sci. Inst. 25, 391 (1954).

26. D. A. Lind, Ph.D. thesis, California Institute of Technology (1948) unpublished.

27. D. A. Lind, W. J. West, and J. W. M. DuMond, Phys. Rev. 77, 475 (1950).

28. E. M. Hatch, Ph.D. thesis, California Institute of Technology (1956) unpublished.

29. A. W. Schardt and J. P. Welker, Phys. Rev. 99, 810 (1955).

30. Grigorev, Zolotavin, Klementev and Sinitzyn, Izvestia Akad. Nauk, SSSR, XXIII, No. 2, 159 (1959).

31. F. R. Metzger and W. B. Todd, Nuclear Phys., 10, 220 (1959).

32. B. R. Mottelson and S. G. Nilsson, Mat. Fys. Skr. Dan. Vid. Selsk. 1 no. 8, (1959).

33. A. K. Kerman,"Nuclear Rotational Motion," in Nuclear Reactions, Vol. 1 (North Holland Publishing Co., Amsterdam) p. 429.

34. C. J. Gallagher, W. F. Edwards, and G. Manning, submitted to Nuclear Phys.

35. Mihelich, Scharff-Goldhaber, McKeown, and McKeown, Phys. Rev. 94, 794A (1954).

36. V. S. Gvozdev and L. I. Rusinov, Akademia Nauk., SSSR, Doklady 112, 401 (1957).

37. M. E. Rose, privately circulated tables of conversion coefficients.

38. M. Vergnes, J. Phys. et Radium 19, 378A (1953).

39. B. I. Spinrad, Phys. Rev. 98, 1302 (1955).

40. J. J. Murray, Ph.D. thesis, California Institute of Technology (1954) unpublished.

41. Alaga, Alder, Bohr and Mottelson, Dan. Mat. Fys. Medd., 29, No. 9 (1955).

42. Gellman, Griffith, and Stanley, Phys. Rev. 85, 944 (1952).

43. P. O. Froman and H. Ryde, unpublished report, University of Lund, Sweden (1956).

44. J. P. Elliott, NYO-2271, University of Rochester, New York (1958).

45. A. W. Schardt and J. P. Welker, Phys. Rev. 99, 810 (1955).

46. A. W. Schardt, Phys. Rev., 108, 398 (1957).

47. H. C. Van den Bold, J. Van de Geijn and P. M. Endt, Physica 24, 23 (1958).

48. W. F. Edwards and C. J. Gallagher, Bull. Am. Phys. Soc. II, No. 4, 279 (1959).

49. A. A. Bashilov and V. V. Il'in, Izvestia Akad. Nauk, SSSR, XXIII, No. 2, 154 (1959).

50. G. Manning and J. Rogers, Nucl. Phys. 15, 166 (1960).

51. W. H. Kelly and M. D. Wiedenbeck, Phys. Rev. 102, 1130 (1956).

52. Cork, Brice, Nester, LeBlanc, and Martin, Phys. Rev. 89, 1291 (1953).

53. Dubey, Mandeville, Mukerji, and Potnis, Phys. Rev., 106, 785 (1957).

54. D. E. Muller, H. C. Hoyt, D. J. Klein and J. W. M. DuMond, Phys. Rev. 88, 775 (1952).

55. Davis, Divatia, Lind, and Moffat, Phys. Rev. 103, 1801 (1956).

56. A. H. Compton and S. K. Allison, X-rays in Theory and Experiment, (D. Van Nostrand Co., New York, 1935) p. 746.